

**SEISMIC PERFORMANCE OF FRICTION DAMPED  
BRACED FRAMES**

**Shamsuddin Mahmoud SABOUNI**



T.C.  
BURSA ULUDAĞ UNIVERSITY  
GRADUATE SCHOOL OF NATURAL AND APPLIED SCIENCES

**SEISMIC PERFORMANCE OF FRICTION DAMPED BRACED FRAMES**

Shamsuddin Mahmoud SABOUNI  
(ORCID : 0000-0001-7489-3938)

Prof. Dr. Hakan Tacettin TÜRKER  
(ORCID : 0000-0001-5820-0257)  
(Supervisor)

MSc THESIS  
DEPARTMENT OF CIVIL ENGINEERING

BURSA – 2023  
All Rights Reserved  
THESIS APPROVAL

This thesis titled “SEISMIC PERFORMANCE OF FRICTION DAMPED BRACED FRAMES” and prepared by Shamsuddin Mahmoud SABOUNI has been accepted as a **MSc THESIS** in Bursa Uludağ University Graduate School of Natural and Applied Sciences, Department of Civil engineering following a unanimous vote of the jury below.

**Supervisor** : Prof. Dr. Hakan Tacettin TÜRKER

<b>Head</b> :	Prof. Dr. Hakan T. TÜRKER (ORCID : 0000-0001-5820-0257) Bursa Uludağ University, Faculty of Engineering, Department of Civil Engineering	Signature
<b>Member:</b>	Dr. Öğr. Üye. Serkan SAĞIROĞLU (ORCID : 0000-0001-7248-3409) Bursa Uludağ University, Faculty of Engineering, Department of Civil Engineering	Signature
<b>Member:</b>	Doç. Dr. Hilmi Coşkun (ORCID : 0000-0003-3667-6945) Faculty of Engineering, Department of Civil Engineering	Signature

**I approve the above result**

**Prof. Dr. Hüseyin Aksel EREN**  
**Institute Director**

.././.....

**I declare that this thesis has been written in accordance with the following thesis writing rules of the U.U Graduate School of Natural and Applied Sciences;**

- All the information and documents in the thesis are based on academic rules,
- audio, visual and written information and results are in accordance with scientific code of ethics,
- in the case that the works of others are used, I have provided attribution in accordance with the scientific norms,
- I have included all attributed sources as references,
- I have not tampered with the data used,
- and that I do not present any part of this thesis as another thesis work at this university or any other university.

**20/06/2023**

**Shamsuddin Mahmoud SABOUNI**

## TEZ YAYINLANMA FİKRİ MÜLKİYET HAKLARI BEYANI

Enstitü tarafından onaylanan lisansüstü tezin/raporun tamamını veya herhangi bir kısmını, basılı (kâğıt) ve elektronik formatta arşivleme ve aşağıda verilen koşullarla kullanıma açma izni Bursa Uludağ Üniversitesi'ne aittir. Bu izinle Üniversiteye verilen kullanım hakları dışındaki tüm fikri mülkiyet hakları ile tezin tamamının ya da bir bölümünün gelecekteki çalışmalarda (makale, kitap, lisans ve patent vb.) kullanım hakları tarafımıza ait olacaktır. Tezde yer alan telif hakkı bulunan ve sahiplerinden yazılı izin alınarak kullanılması zorunlu metinlerin yazılı izin alınarak kullandığımı ve istenildiğinde suretlerini Üniversiteye teslim etmeyi taahhüt ederiz.

Yükseköğretim Kurulu tarafından yayınlanan “**Lisansüstü Tezlerin Elektronik Ortamda Toplanması, Düzenlenmesi ve Erişime Açılmasına İlişkin Yönerge**” kapsamında, yönerge tarafından belirtilen kısıtlamalar olmadığı takdirde tezin YÖK Ulusal Tez Merkezi / B.U.Ü. Kütüphanesi Açık Erişim Sistemi ve üye olunan diğer veri tabanlarının (Proquest veri tabanı gibi) erişimine açılması uygundur.

Prof. Dr. Hakan Tacettin TURKER  
Danışman Adı-Soyadı  
Tarih

Oğrencinin Adı-Soyadı  
Tarih

İmza  
Bu bölüme kişinin kendi el yazısı ile okudum anladım  
yazmalı ve imzalanmalıdır.

İmza  
Bu bölüme kişinin kendi el yazısı ile okudum  
anladım yazmalı ve imzalanmalıdır.

## ÖZET

Yüksek Lisans Tezi

### SÜRTÜNME TİPİ SÖNÜMLEYİCİLİ YAPILARIN SİSMİK PERFORMANSI

**Shamsuddin Mahmoud SABOUNI**

Bursa Uludağ Üniversitesi  
Fen Bilimleri Enstitüsü  
İnşaat Mühendisliği Anabilim Dalı

**Danışman:** Prof. Dr. Hakan Tacettin TÜRKER

Sürtünme tipi sönümleyici deprem etkisi ile oluşacak enerjiyi sönümleyerek yapıda oluşacak deprem kaynaklı kuvvetlerin etkilerini azaltmak için iki yüzey arasındaki sürtünmeyi kullanan yapısal bir cihazdır. Bu cihazlar bir çapraz elemanla birlikte moment aktaran çerçeve sistemlere bağlanır ve yük aktarımını bu şekilde gerçekleştirir.

Bu çalışmanın amacı, sürtünme tipi sönümleyici cihazların moment aktaran çelik çerçeve sistemler üzerindeki davranışına etkisini incelemektir. Bu çalışmada doğrusal olmayan statik itme ve zaman tanım alanında doğrusal olmayan analiz yöntemleri kullanılmıştır. Kıyalasmalar için literatürden 4 ve 9 katlı iki adet moment aktaran çelik çerçeve seçilmiştir. Yapılara önce sürtünme tipi sönümleyici ve ardından çapraz eleman eklenmiştir. Yapılan araştırmalarda maksimum tepe yerdeğiştirmesi, maksimum kat kesme kuvvetleri, görelî kat ötelenme oranları ve taban kesme kuvvetleri incelenmiştir.

Sonuçlar, yapıların sismik performansının etkili bir şekilde iyileştirebileceğini ve bu tür sistemlerin tasarımı ve optimize edilmesi konusunda değerli bilgiler sunabileceğini göstermektedir.

**Anahtar Kelimeler:** Sürtünme Sönümleyicisi, Zaman tanım alanında doğrusal olmayan analiz, İtme Analizi, Moment aktaran Çelik Çerçeve, Sürtünme Sönümlenmeli Çapraz

## **ABSTRACT**

MSc Thesis

### **SEISMIC PERFORMANCE OF FRICTION DAMPED BRACED FRAMES**

**Shamsuddin Mahmoud SABOUNI**

Bursa Uludağ University  
Graduate School of Natural and Applied Sciences  
Department of Civil Engineering

**Supervisor:** Prof. Dr. Hakan Tacettin TÜRKER

Friction-damped braced frames are a type of structural system that utilizes friction between two surfaces to dissipate energy and reduce seismic forces on the structural components of buildings. These frames consist of diagonal braces connected to the beams and columns of a building, with friction dampers inserted as a part of the brace.

The objective of this study is to investigate and improve the seismic behavior of moment-resisting frame structures by employing friction-damped braces. The analysis methods utilized in this study include time history analysis and pushover analysis. The research involves a comparative analysis of three different framing systems: moment-resisting frame (MRF), braced frame (BF), and friction-damped braced frame (FDBF). The comparison is based on evaluating different parameters such as top displacement, story drifts, shear forces, and base shear values. Two moment-resisting frames were selected in this investigation. The first frame comprises four stories with four bays, while the second frame consists of nine stories with five bays.

Using time history analysis and pushover analysis, the seismic performance of the framing systems is thoroughly examined and compared. This comprehensive evaluation provides insights into the advantages and limitations of each framing system in terms of their response to seismic excitations. The results demonstrate that friction-damped braces can effectively improve the seismic performance of buildings and provide valuable insights into the design and optimization of such systems.

**Keywords:** Friction Damper, Nonlinear Time-history Analysis, Pushover Analysis, Moment Resisting Steel Frame, Friction Damped Brace.

## **ACKNOWLEDGMENT**

First and foremost, I would like to express my deepest gratitude to my thesis supervisor Professor. Dr. Hakan Tacettin TÜRKER, for their invaluable guidance, support, and encouragement throughout the entire research process. Their expertise, insights, and constructive feedback have been instrumental in shaping the direction of this thesis.

My sincere thanks go to my family, especially my parents for their unwavering support, encouragement, and love throughout my academic journey. Their sacrifices, patience, and understanding have been a source of strength and motivation throughout the ups and downs of this process.

Finally, I would like to express my gratitude to the Turkish scholarship and to all the participants who took part in this research. Without their support and encouragement, this work would not have been possible.

Shamsuddin M. SABOUNI  
20/06/2023.



## CONTENTS

	<b>Page</b>
ÖZET.....	i
ABSTRACT.....	ii
ACKNOWLEDGMENT.....	iii
SYMBOLS and ABBREVIATIONS.....	v
FIGURES.....	vii
TABLES.....	x
1. INTRODUCTION.....	1
1.1 GENERAL.....	1
1.2 ORGANIZATION OF THE THESIS.....	2
2. THEORETICAL BASICS and LITERATURE REVIEW.....	4
2.1 Friction Dampers.....	4
2.1.1: Slotted-Bolted Connections.....	5
2.1.2: Sumitomo Friction Damper.....	9
2.1.3: Pall Friction Damper PFD.....	10
Applications of PFD.....	14
2.1.4: Rotational Friction Damper RFD.....	17
2.3 Friction Damped Braced Frames FDBF.....	19
2.4: Previous Studies and Research.....	22
3. MATERIALS and METHODS.....	26
3.1 Building Model.....	26
3.1.1 System Description.....	26
3.1.2 Loads applied on systems.....	29
3.1.3. Earthquake parameters.....	31
3.2. Nonlinear modelling and analysis.....	32
3.2.1. Modeling of Plastic Hinge.....	32
3.2.2 Nonlinear static (pushover) analysis.....	36
3.2.3 Time history analysis.....	41
3.3 Slip Load and Stiffness of the FDBs.....	42
4. RESULTS AND DISCUSSION.....	45
4.1. Period and Frequency values.....	45
4.2. Slip load and stiffness of braces.....	46
4.3 Comparison of Top Displacements.....	47
4.4 Comparison of Relative Story Drifts.....	50
4.5 Comparison of Shear Forces.....	52
4.6 Pushover (Capacity) Curves.....	56
4.7 Plastic Hinges State.....	57
5. CONCLUSION.....	63
REFERENCES.....	65
RESUME.....	68

## SYMBOLS and ABBREVIATIONS

<b>Symbols</b>	<b>Definition</b>
$m$	The mass of the system
$S_d$	Spectral displacement
$S_a$	Spectral acceleration
$T$	Time period
$g$	Gravity acceleration
$W$	Total weight of the system
$G$	Dead Load
$Q$	Live Load
$S_1$	Largest Considered Earthquake's spectral acceleration at one second
$K$	Stiffness of the structure
$I_c$	Moment of inertia for Columns
$I_b$	Moment of Inertia for Beams
$M_{pc}$	Yield moment of columns
$M_{pb}$	Yield moment of the beam
$F_y$	Yield stress
$E$	Young's modulus of elasticity
$V_b$	Shear resisted by the damped brace
$V_f$	Shear resisted by the damped frame
$P_s$	Slip load of the brace
$\phi$	The angle between the beam and brace
$h$	Height of the floor
$L$	The width of the frame
$K_b$	The stiffness of the brace
$K_f$	Stiffness of the brace
$\rho$	Stiffness ratio of beam/column
$\lambda$	Stiffness ratio of brae/frame
$K_{FDBF}$	Stiffness of FDBF
$K_{MRF}$	Stiffness of MRF
$\omega_F$	First natural frequency of FDBF
$\omega_m$	First natural frequency of MRF
$n$	The number of bays in the frame

<b>Abbreviation</b>	<b>Definition</b>
FDB	Friction damped brace
MRF	Moment resisting frame
BF	Braced frame
FDBF	Friction damped braced frame
MPA	Modal pushover analysis
IMPA	Improved modal pushover analysis
MDOF	Multi-degree-of-freedom
SDOF	Single-degree-of-freedom
PFD	Pall friction damped
RFD	Rotational friction damper
CBF	Centrically braced frame
BRC	Buckling restrained column
SBC	Slotted-bolted connection
AFC	Asymmetric friction connection
SFC	Symmetric friction connection
NL-RHA	Nonlinear response history analysis
TSCB	Turkish Seismic Code for Buildings

## FIGURES

	<b>Page</b>
Figure 2.1. Sliding surface of steel plates in a friction damper .....	4
Figure 2.2. Slotted-Bolted Connections a) slotted-bolted connection configuration. B) slotted bolted connection details (Fitzgerald et al. 1989).....	5
Figure 2.3. Frame equipped with SBC in diagonal brace (Grigorian et al., 1993).....	6
Figure 2.4. Types of Slotted-bolted Connections a) Symmetrical Friction Connection SFC b) Asymmetric Friction Connection AFC (Robin Xie 2019).....	7
Figure 2.5. SFC. a) Typical layout of SFC b) its application in RSBC c) force-displacement behavior (Hsen-Han Khoo 2014, ShahabRamhormozian 2017).....	8
Figure 2.6. AFC. a) Typical layout of AFC b) its application in Sliding Hinge Joint c) force-displacement behavior (Yeung S 2013, Shahab Ramhormozian 2017).....	8
Figure 2.7. Sumitomo-Type Friction Damper Device a) General layout of the damper b) Its installation in the construction system (Ercan Atam, 2019).....	9
Figure 2.8. Friction Dampers a) Single diagonal brace b) Hysteresis loop for PFD c) Cross bracing PFD system (Pall and Pall 2004).....	10
Figure 2.9. Pall friction damper details, Cross bracing type (Seyed Zahraei, 2013).....	11
Figure2.10 An idealized description of a one-story friction-damped frame's hysteretic behavior (Cherry s, 1993).....	12
Figure2.11 Friction damper`s slip load versus Response (Pall and Pall, 2004).....	13
Figure2.12 Improving the seismic resistance of the Boeing Commercial Airplane Factory by PFDs, Everett, Washington, USA (Pall and Pall, 2004).....	14
Figure2.13 Moscone West Convention Center equipped with PFDs, San Francisco, USA (Pall and Pall, 2004) .....	14
Figure2.14 Providing PFDs for the Cafeteria and Auditorium Buildings in Boeing Development Center, Boeing Field, Seattle, WA, USA (Pall and Pall, 2004).....	15
Figure2.15 The use of PFDs in Provincial Police Headquarters in Quebec, Montreal, Canada (Pall and Pall, 2004).....	15
Figure2.16 Three-Million Gallon Reservoir equipped with PFDs, Sacramento, California, USA (Pall and Pall, 2004).....	15
Figure2.17 Concordia University Library Building with the addition of PFDs, Montreal, Canada (Pall and Pall, 2004).....	16
Figure2.18 A view of Sharp Memorial Hospital's ambulatory care center with PFDs, San Diego, California, USA Response (Pall and Pall, 2004).....	16

Figure2.19	General View of St. Joseph medical center patient tower with PFDs (Shao et al., 2006).....	16
Figure2.20	Details of the RFD device suggested by Mualla and Belev (Mualla and Belev, 2002).....	17
Figure2.21	The RFD's operating system (Mualla and Belev, 2002).....	18
Figure2.22	Hysteretic behavior of a friction-damped steel brace .....	19
Figure 3.1.	Plan and side view and floor heights of the 4-story steel structure ...	27
Figure 3.2.	Plan and side view and floor heights of the 9-story steel structure ...	28
Figure 3.3.	Vertical loads acting on the MRF in a 4-storey system .....	30
Figure 3.4.	Lateral elastic design response spectrum (TSCB 2018).....	32
Figure 3.5.	Generalized Force Displacement Curve (FEMA 356).....	33
Figure 3.6.	Moment-rotation relationship of HE700A element in Sap 2000.....	34
Figure 3.7.	Axial force-moment relationship in Sap 2000 program .....	34
Figure 3.8.	Moment-rotation relationship at 20% axial force capacity level in Sap 2000 program .....	35
Figure 3.9.	Moment-rotation relationship at 80% axial force capacity in Sap 2000 program .....	35
Figure3.10	Nonlinear static (Pushover) analysis method .....	36
Figure3.11	Global Capacity Curve of The Structure (Pushover Curve).....	37
Figure3.12	Non-linear vertical loading combination .....	39
Figure3.13	Equivalent earthquake load calculation of Sap2000 program according to TSCB 2018.....	40
Figure3.14	Parameters of Pushover analysis of the structure in Sap2000 program .....	40
Figure3.15	Plastic hinge properties of FDB in first floor of 4-story FDBF system .....	44
Figure3.16	Plastic hinge properties of FDB in first floor of 9-story FDBF system .....	44
Figure 4.1.	Comparison of roof displacements of 4-story frames under different ground motions a) RSN 983 b) RSN 1013 c) RSN 8164.....	48
Figure 4.2.	Comparison of roof displacements of 9-story frames under different ground motions a) RSN 983 b) RSN 1111 c) RSN 4456.....	49
Figure 4.3.	Comparison of Relative story drift ratios of 4-story frames under different ground motions a) MRF b) BF c) FDBF .....	51
Figure 4.4.	Comparison of Relative story drift ratios of 9-story frames under different ground motions a) MRF b) BF c) FDBF .....	51
Figure 4.5.	Comparison of average values of relative story drifts % under different ground motions for all frames a) 4-story frames b) 9-story frames .....	52
Figure 4.6.	Comparison of shear force values under different ground motions applied on 4-story frames a) MRF b) BF c) FDBF .....	53
Figure 4.7.	Comparison of shear force values under different ground motions applied on 9-story frames a) MRF b) BF c) FDBF .....	54
Figure 4.8.	Comparison of average values of shear forces under different ground motions for all frames a) 4-story frames b) 9-story frames...	55
Figure 4.9.	Comparison between pushover curves (capacity curves) for all frames a) 4- Story frames b) 9-Story frames .....	56

Figure4.10	Last state of plastic hinges under RSN 983 ground motion for all 4-story frames a) MRF b) BF c) FDBF .....	57
Figure4.11	Last state of plastic hinges under RSN 1013 ground motion for all 4-story frames a) MRF b) BF c) FDBF .....	58
Figure4.12	Last state of plastic hinges under RSN 8164 ground motion for all 4-story frames a) MRF b) BF c) FDBF .....	59
Figure4.13	Last state of plastic hinges under RSN 983 ground motion for all 9-story frames a) MRF b) BF c) FDBF .....	60
Figure4.14	Last state of plastic hinges under RSN 1111 ground motion for all 9-story frames a) MRF b) BF c) FDBF .....	61
Figure4.15	Last state of plastic hinges under RSN 4456 ground motion for all 9-story frames a) MRF b) BF c) FDBF .....	62

## TABLES

	<b>Page</b>
Table 3.1. Geometric properties of the selected structures .....	26
Table 3.2. ASTM A991 Grade 50 material properties .....	29
Table 3.3. Loads acting on structures .....	29
Table 3.4. Distributed load acting on beams .....	30
Table 3.5. Normal load acting on columns .....	30
Table 3.6. Values of vertical loads acting on 4 story MRF.....	31
Table 3.7. Earthquake parameters .....	31
Table 3.8. Earthquake records selected for the 4-story structure .....	41
Table 3.9. Earthquake records selected for the 9-story structure.....	42
Table 4.1. Values of Period and Frequency for first three modes of 4- story MRF, BF, and FDBF .....	45
Table 4.2. Values of Period and Frequency for first three modes of 9- story MRF, BF, and FDBF .....	46
Table 4.3. Values of slip forces and brace sections for 4-story systems.....	46
Table 4.4. Values of slip forces and brace sections for 9-story systems .....	47
Table 4.5. Values of top displacements for all systems .....	50

# **1. INTRODUCTION**

## **1.1 GENERAL**

In recent decades, many researchers in Turkey and elsewhere are trying to develop ways that would raise the efficiency of structural systems to resist earthquakes. One of these methods, which appeared in the early eighties of the last century, was friction-damped braces (FDBs) that were added to the structural system, such as moment-resisting frames (MRFs). This was the starting point for the development of friction dampers technology, which spread globally and is still spreading until the present time. Friction-damped braced frames offer an innovative approach to dissipate energy and reduce seismic forces on structural components. These frames incorporate diagonal braces connected to beams and columns, with friction dampers inserted as part of the braces. The friction mechanism allows the energy generated during an earthquake to be absorbed and dissipated, thereby reducing the overall demand on the building.

The objective of this thesis is to investigate and improve the seismic behavior of moment resisting frame structures through the implementation of friction-damped braces. By employing rigorous analysis methods such as time history analysis and pushover analysis, the seismic performance of three framing systems will be compared: moment resisting frame (MRF), braced frame (BF), and friction-damped braced frame (FDBF). The comparative analysis will consider key parameters including top displacement, story drifts, shear forces, and base shear values to evaluate the effectiveness of the different framing systems under seismic excitations.

To provide a comprehensive evaluation, two moment-resisting frames have been selected as case studies. The first frame consists of four stories with four bays, while the second frame comprises nine stories with five bays. Through a systematic examination of these frames and comparison of the three framing systems, valuable insights will be gained into the advantages and limitations of friction-damped braces in improving the seismic performance of buildings.



## **1.2 ORGANIZATION OF THE THESIS**

### **CHAPTER 1. INTRODUCTION**

This chapter of the thesis represents a general introduction to the topic of the thesis and a simplified definition of the methods of analysis and the structural systems used in the investigation.

### **CHAPTER 2 THEORETICAL BASICS AND LITERATURE REVIEW**

This chapter represents a detailed explanation of friction dampers and their main types, including an explanation of each type separately, in addition to the importance of FDBFs as well as previous studies such types of dampers with methods of analysis used in these studies.

### **CHAPTER 3 MATERIALS AND METHOD**

This chapter of the dissertation presents the most important theoretical part, as it deals with the methods of analysis used: nonlinear dynamic analysis or time history analysis in addition to nonlinear static analysis or pushover analysis method. modeling of selected steel frames with different number of stories is shown using finite element program (SAP2000). The chapter deals with a description of the structural systems selected in this study and loading applied to the systems and earthquake parameters. Finally, the approach to calculate the optimum slip load for FDBs and stiffness of braces is also included in this chapter.

### **CHAPTER 4 RESULTS AND DISCUSSION**

This chapter of the dissertation presents the detailed analysis results that were extracted from the selected analysis program. It includes the results extracted from nonlinear time

history analysis as well as pushover analysis. The results are evaluated and compared with the goal of evaluating the seismic performance of moment-resisting frames and the frames supported by diagonal braces and friction-damped braces.

## **CHAPTER 5 CONCLUSION**

This last chapter of the thesis represents a comprehensive summary and conclusion of the thesis and the most important outputs and findings.

## 2. THEORETICAL BASICS and LITERATURE REVIEW

### 2.1 Friction Dampers

Friction dampers are considered as a type of Passive Control Systems that requires no power to operate. This kind of dampers began to be used in civil engineering structures in the last quarter of the last century. These dampers have been developed over the past years to improve the seismic response of buildings. They rely on the friction mechanism, which has been used in many fields since ancient times to regulate the movement of objects. The types of friction dampers may differ in their characteristics and design; however, they all have the same working mechanism as they dissipate seismic energy through frictional sliding at the interfaces of two or more elements (Figure 2.1). Frictional force (resistive force) arises due to the relative motion of solid surfaces attached to each other. These dampers are widely used to reduce the kinetic energy of moving objects as they are the most effective, reliable, and inexpensive in cost (Pall and Pall 1996).



**Figure 2.1.** Sliding surface of steel plates in a friction damper.

During a strong seismic motion, the damper actually starts to operate at a predetermined friction force called (Slip Load) that should be reached in order to allow the plates to slip and for the purpose of dissipating seismic energy via friction. Friction dampers maintain their properties during thermal fluctuations and have a constant hysterical behavior with high performance during strong earthquake motions (Filiatrault et al., 1987).

It can be said that the main types of friction dampers are as follows:

- Slotted-Bolted Connections
- Sumitomo Friction Damper
- Pall Friction damper
- Rotational Friction Damper

### 2.1.1: Slotted-Bolted Connections

Slotted-bolted Connections (SBC) were suggested by Fitzgerald et al. (1989) after noticing some limitations in Pall's device including the inelastic buckling of the brace and the low activation force. SBCs are one of the main types of damper devices which is intended to dissipate seismic energy via friction. These connections consist of a steel gusset and cover plates, connected by steel bolts with a washer passing through successive channels that absorb seismic energy through friction surfaces. The benefit of using a washer is to prevent any form of failure such as yielding or buckling of the members during the sliding process between the plates. Slotted-bolted connection configuration is illustrated in Figure 2.2 (a, b).

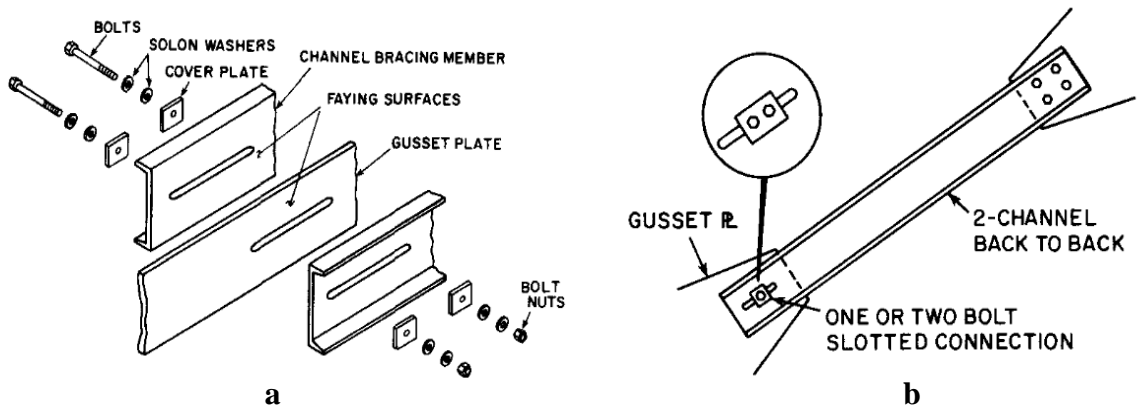


**Figure 2.2.** Slotted-bolted connections **a)** slotted-bolted connection configuration. **b)** slotted bolted connection details (Fitzgerald et al. 1989).

SBCs are easy to manufacture as they do not require exotic materials and do not require precision parts during construction and that gives them an advantage over many alternatives (Grigorian et al., 1993). The diagonal brace can be seen in Figure 2.3 which is attached to the two ends of the frame by connections. The SBC device is located at one end of the brace. It is connected to the frame through one end and to the brace through the other one. Grigorian et al 1993 studied this type of devices in their doctoral thesis in an analytical and experimental research. Where the results of his investigation concluded in two main parts: the first part was dealing with the SBCs themselves, the way they are installed, and their properties. While the second part was focusing on the structural systems of these connections as a primary cause of dissipated energy.

Grigorian noticed that during seismic events, slipping occurred at the contact face between the gusset plate and the damping device. The relative motion between the two sliding elements produces friction by which seismic energy is controlled. The research shows that if the device is well designed, it can be installed in structural systems as a very efficient means of energy dissipation during earthquakes.

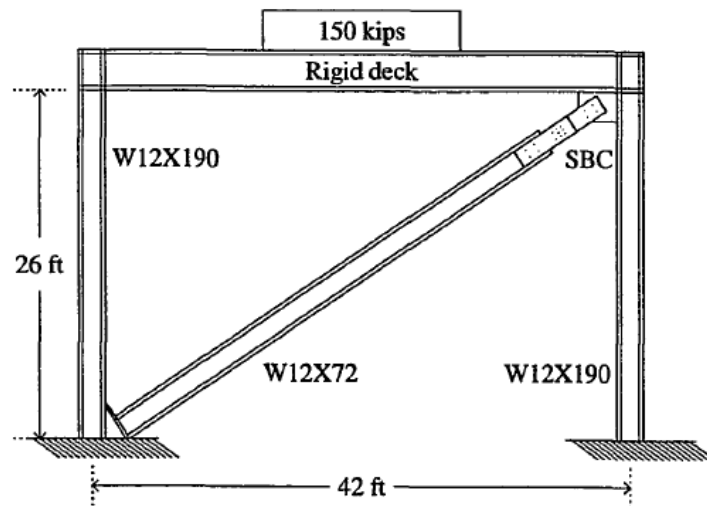


**Figure 2.3.** Frame equipped with SBC in diagonal brace (Grigorian et al., 1993).

A slotted-bolted connection must be able to withstand multiple cycles of displacement without losing strength, stability, or energy dissipation capabilities. The effective performance of SBC's sliding is significantly influenced by a number of important parameters, including:

- Maintaining the contact pressure between sliding surfaces of steel plates
- Preservation of an almost constant coefficient of friction between sliding surfaces
- Preventing brittle failure of any connection at the point where the connection's sliding range is at its maximum.
- Maintenance and construction are easy and inexpensive.

In general, two different types of SBCs are existing and they could be appropriate for a structural frame's bracing system. The first one is called **Symmetrical Friction Connection (SFC)** while the other type is **Asymmetric Friction Connection (AFC)**.

Figure 2.4 provides a straightforward explanation that demonstrates the essential characteristics of an AFC and SFC. These two friction devices are both made up of a number of plates that are connected together using high-tensile bolts. One of the plates in each of these devices has long slots carved into it, allowing it to transfer external stress via the connection details. This plate is known as a slotted plate. The friction connection is frequently connected to a main structural part, such as a column, beam, or bracing member, using a fixed plate. The slotted plate tends to slide over a distance equal to the length of the slots with little force increases after the external load \_generated by an earthquake\_ surpasses the clamping force given by the bolts.

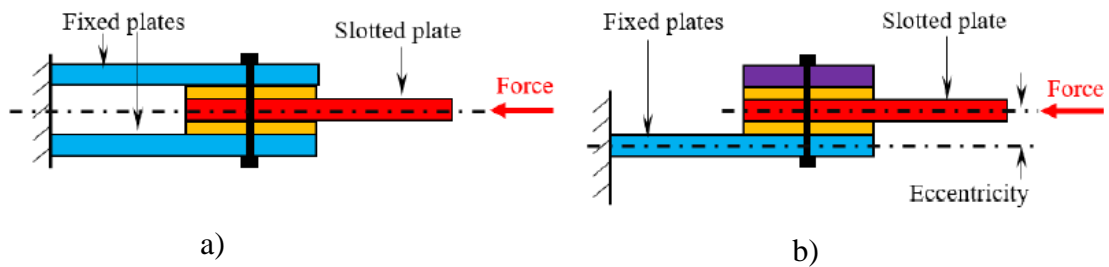


**Figure 2.4.** Types of Slotted-bolted Connections. **a)** Symmetrical Friction Connection SFC **b)** Asymmetric Friction Connection AFC (Robin Xie 2019).

The main distinction between the two types of SBC is that an AFC has an asymmetrical alignment, which causes the load to be eccentrically transmitted to the fixed plate from the slotted plate and then transferred to the adjacent component when the load is applied at the midline of the slotted plate. The AFC experiences a moment due to the eccentricity, which might lead it to deflect out of the plane along with the adjacent sub-system. An SFC, on the other hand, employs a symmetrical alignment to allow the external force to be transmitted concentrically to the structural element to which the SFC is attached.

There are two primary sliding interfaces in the AFC. The cleat's interaction with the top shim is the first, while its interface with the lower shim is the second. The system starts to slide after the applied force surpasses the initial AFC sliding interface's frictional resistance. The AFC bolts are forced into the double curvature condition, also known as the stable sliding state, after a short stage of sliding. When the load is reversed, the same behavior occurs, but in the other direction. This AFC behavior is the result of the AFC

having a partially floating cap, and it gives the Sliding hinge joint, or any system incorporating the AFC, a "pinched" hysteretic curve. This curve is more akin to a flag-shaped hysteresis curve than an SFC assemblage square curve.

The force-displacement behavior of the SFC is less complex than the AFC. The two primary sliding interfaces of the SFC are between the plate in the middle and upper and lower shims, or, if the outside plates have slotted holes, between the outer plates and two layers of shims, as well as under the bolt head and nut. In an ideal situation, the bolts are only under tension force for the slotted middle plate with SFC and under tension, shear, and bending moment with slotted outer plates when the applied force reaches the frictional resistance force of both SFC sliding interfaces and the sliding of the system begins. This offers an idealized rectangular hysteretic curve to the SFC. Part (a) in Figures 2.5 and 2.6 shows the typical layout of SFC and AFC respectively. Part (b) of the same figures describes their applications. While (c) part illustrates the ideal force-displacement behavior for both types of SBC.

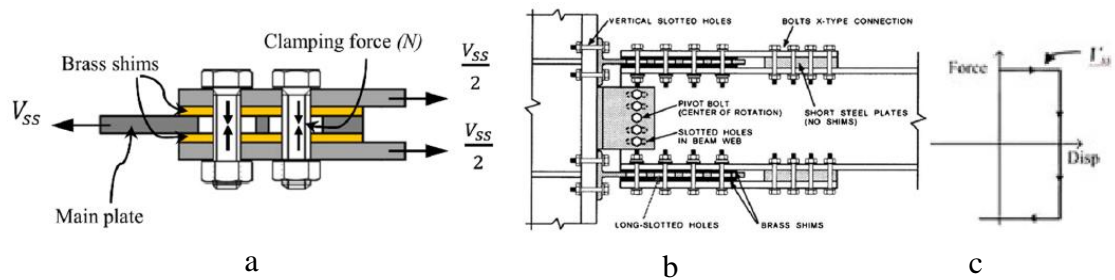


**Figure 2.5.** SFC. **a)** Typical layout of SFC **b)** its application in RSBC **c)** force-displacement behavior (Hsen-Han Khoo 2014, ShahabRamhormozian 2017).

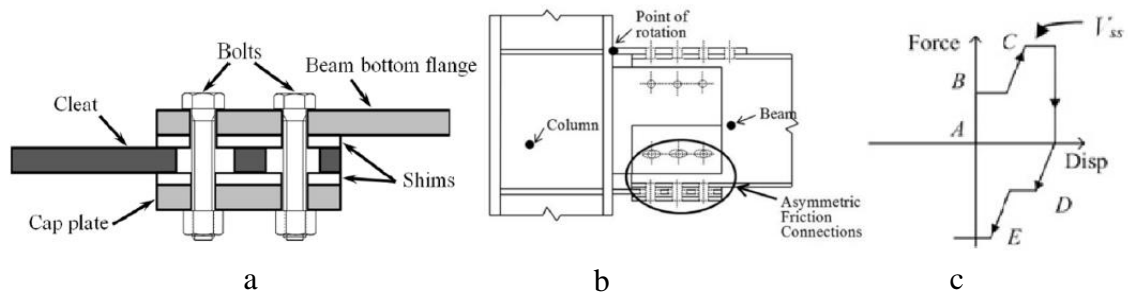


**Figure 2.6.** AFC. **a)** Typical layout of AFC **b)** its application in Sliding Hinge Joint **c)** force-displacement behavior (Yeung S 2013, Shahab Ramhormozian 2017).

### 2.1.2: Sumitomo Friction Damper

Sumitomo Metal Industries Ltd in Japan created and developed a different friction damper device used as a shock absorber in railway applications, called Sumitomo Friction Damper. In order to develop the Sumitomo device, the Earthquake Research Center in Berkeley conducted an experimental test using it as a passive energy dissipator. The cylindrical instrument has copper alloy friction pads that move over the inside case's steel surface (Towashiraporn et al., 2002). Friction occurs between friction pads and the inside surface of the steel, which produces the frictional force. This dissipation device is positioned parallel to the beams. It is divided into two segments, one of them attached to a floor beam, and the other one attached to a chevron bracing system. Figure 2.7 represents how these dissipation segments are arranged within the structures.

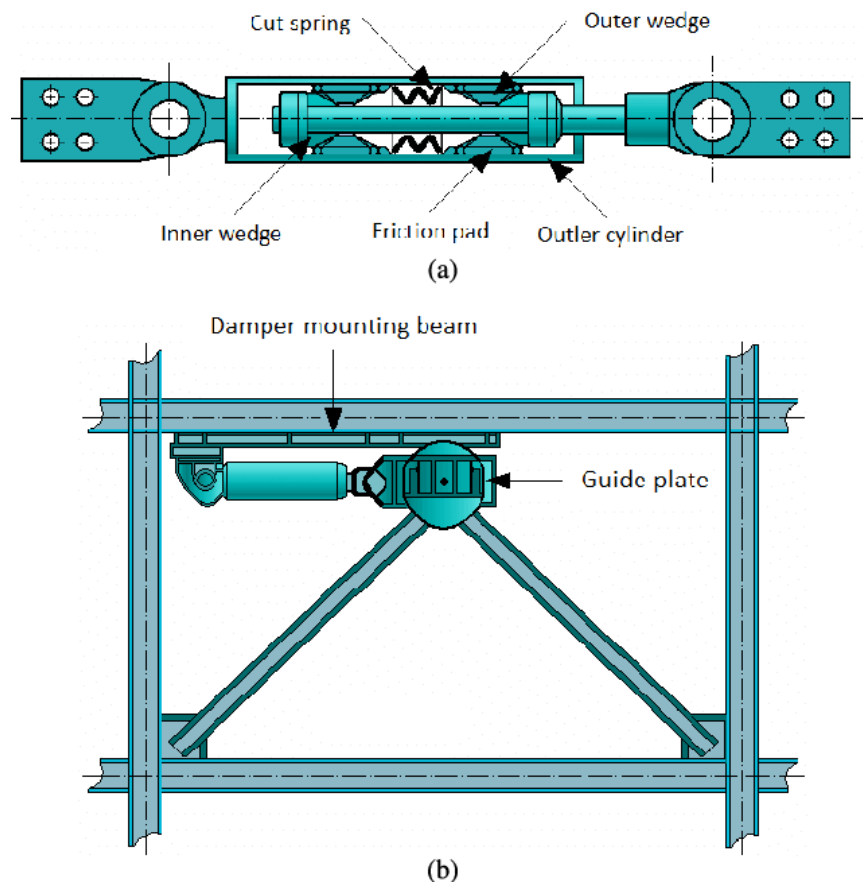


**Figure 2.7.** Sumitomo-type friction damper device **a)** General layout of the damper **b)** Its installation in the construction system (Ercan Atam, 2019).



### 2.1.3: Pall Friction Damper PFD

The major operating concept of the passive energy dissipating systems discussed before depends on the friction mechanism, and the most used friction damper type is Pall Friction Damper PFD. In the past, researchers and engineers created mechanical and structural systems employing this mechanism, particularly in the braking systems of motor vehicles and ultimately in the construction of structures. Their target was to use a friction mechanism to absorb the kinetic energy. It can be realized that with the development of the PFDs at the year of 1979, researchers made significant advances in their efforts to absorb seismic energy. PFD has been used widely to minimize the impact of earthquake damage and these dampers are sufficient for success in the seismic design of structures globally (Pasquin et al., 2002).

PFD might be viewed as a more advanced new version of Slotted-Bolted Connections SBCs. The basic operating principle is comparable to SBC and relates to relative sliding between surfaces in contact. The friction force that results relies on surfaces in touch with the brake lining pad that is held together by high-strength screws post-tensioned. PFD is constructed of steel plates that can slide when subjected to a specific design load. It is possible to use pall friction dampers as a single diagonal tension-compression bracing system, or tension-only cross bracing system as seen in Figure 2.8.

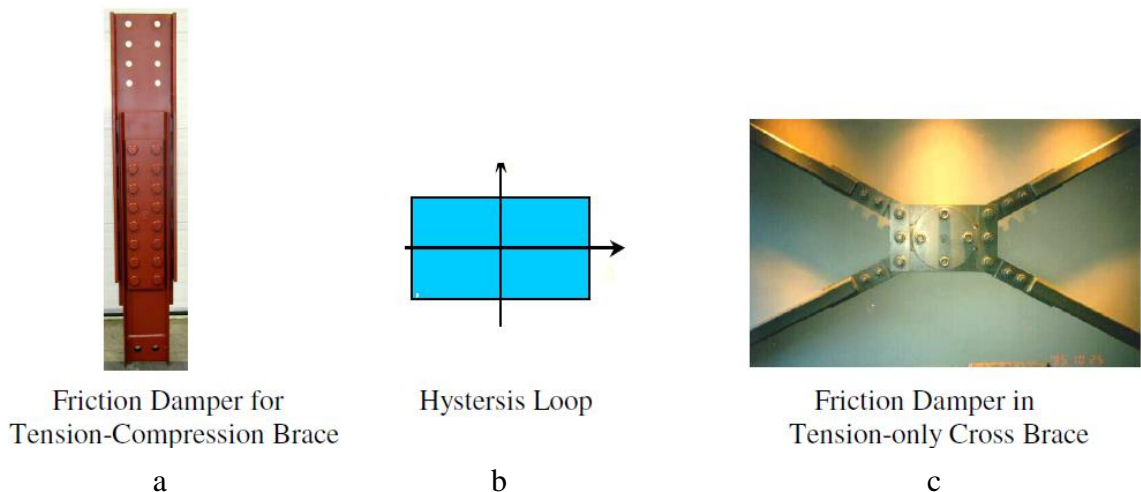


**Figure 2.8.** Friction dampers **a)** Single diagonal brace **b)** Hysteresis loop for PFD **c)** Cross bracing PFD system (Pall and Pall 2004).

The mechanism used for the cross-bracing system is special which is illustrated in Figure-2.9. When the damper slips due to one of the tensioned braces, the damper mechanism pushes the other brace to shorten in order to prevent buckling. When the cycle is reversed in this way, the opposite brace is instantly prepared to slide the damper (pall and pall, 2014). Pall Friction Connectors are specifically designed to allow for bidirectional motions to prevent pounding at the expansion joints.

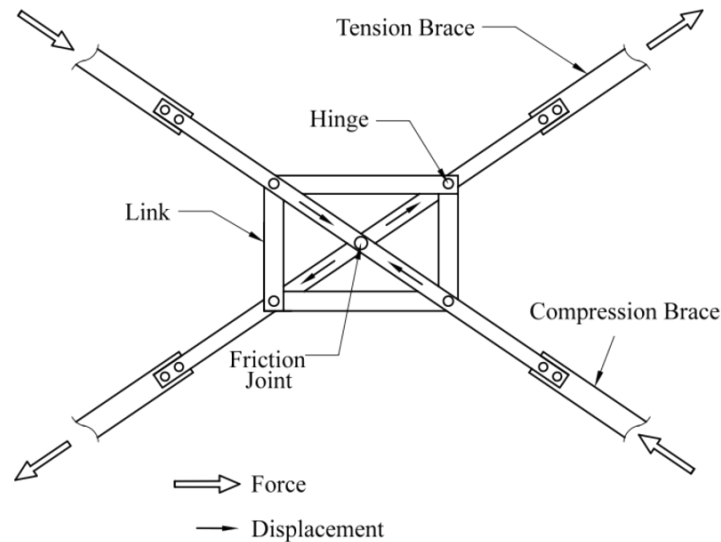


**Figure 2.9.** Pall friction damper details, cross bracing type (Seyed Zahraei, 2013).

The five phases of the pall friction dampers' behavior during a typical load cycle are depicted in Figure 2.10, as well as the deformed shape of the frame at each phase. Following is a description of how the frame member responded at each step:

First step: both braces are functioning and respond elastically to compression and tension forces.

Second step: While the tension brace keeps acting elastically in tension, the compression brace starts to buckle.

Third step: The device is supposed to slide before yielding is initiated in the tension brace. The compression brace's buckling is eliminated by the activation of the four links, which deform into a rhomboid shape when slippage occurs. As a result, even after slippage, the

compression brace is still straight and its axial force is equivalent to the load that would cause it to buckle.

Fourth step: When the load is reversed, the straightened brace may directly absorb energy in tension.

Fifth step: Once the load in the first brace exceeds the buckling load, The second step is repeated. The other steps then come, and the cycle continues (Cherry s, 1993).

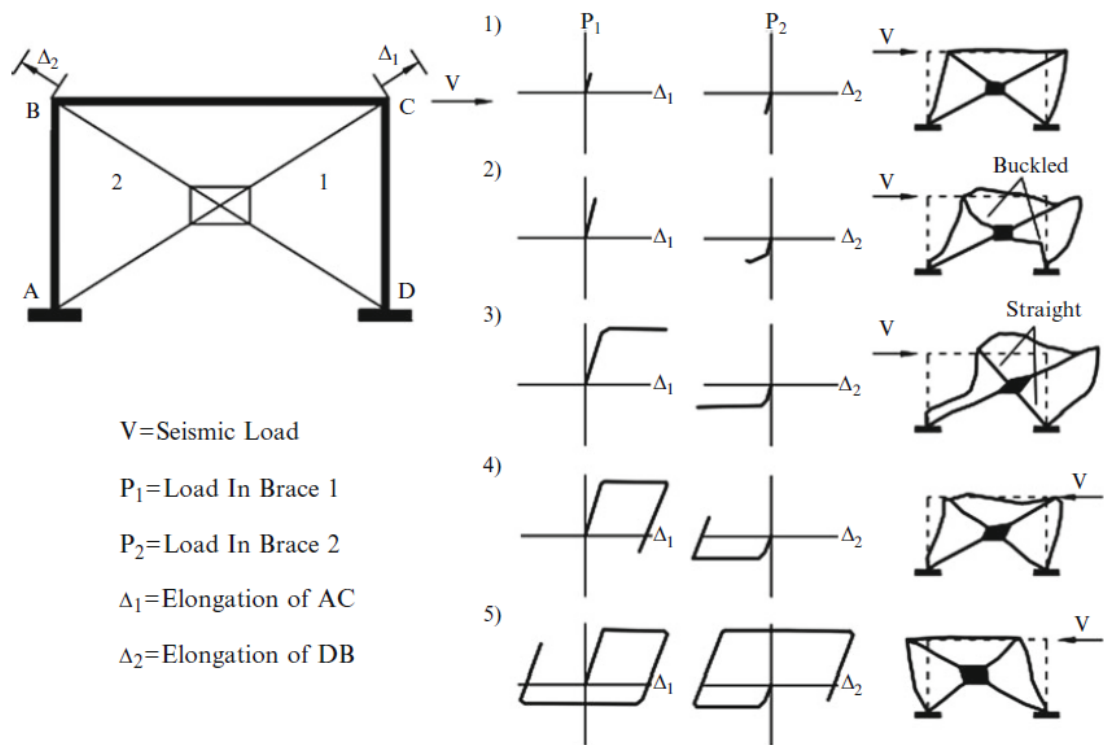


**Figure 2.10.** An idealized description of a one-story friction-damped frame's hysteretic behavior (Cherry s, 1993).

There are many benefits to using PFDs, the most prominent of which are the following:

- Their construction is easy and reliable with repeatable performance at low cost.
- Big rectangular hysteresis loops are present. increased energy loss for a given force. It follows that less number of PFDs are required. Alternately, use less force for the same dampening.
- When there are service loads and wind, they are inactive. Therefore, there is no chance of failure due to fatigue before any seismic action.

- Before and after the seismic action, no repairs or replacements are required.
- Forces and deflections are reduced when strong damping is introduced.
- Making the structure, its contents, and its people safer.
- Low-cost design of the damper based on performance.
- As damage is controlled, life cycle costs are reduced.
- Cost savings for both new constructions by up to 1-2% and retrofitting existing structures by 30-60%.

The bracing of structures appears to buckle in the case of compression loads and yield under tension loads. However, it is envisaged that PFD connection components will yield in both tension and compression conditions. PFDs slide before the yielding of structural elements during a strong earthquake. They begin to move and dissipate the seismic energy when the lateral loads equal the designed slip load value. The slip load designation becomes the most critical factor in the design of PFD as a result of this event. As shown in Figure 2.11, the response seems to be quite high whether the slip load is very small or very big. The minimum response is produced by the optimum slip load. The design of the slip load should also guarantee that, after seismic action, the building will return to its almost original alignment. PFD does not slide if the slip load is too low, and the quantity of energy dissipated is at a limited level.

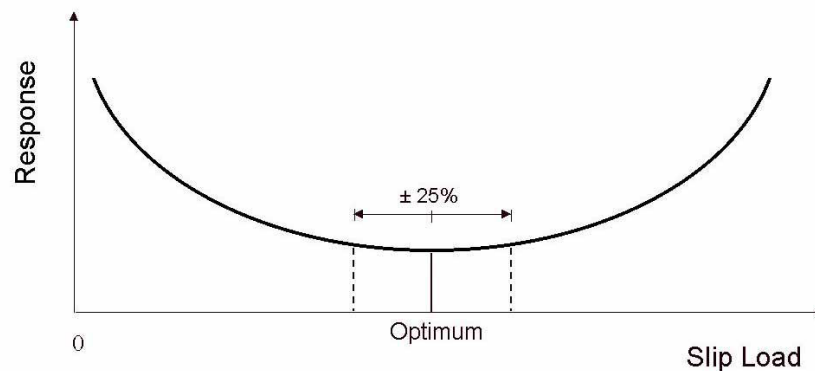


**Figure 2.11** Friction damper`s slip load versus Response (Pall and Pall, 2004).

## Applications of PFD

(Pall and Pall, 2004) presented some applications of PFDs in his article. According to him, this type of damper was first used in 1987 in North America for the Concordia University Library Building composed of a 10-story concrete structure. PFDs are being used more often in new construction and building retrofits across the world, including water tanks overhead. More than 80 types of structures in Canada, the U.S., India, and China have utilized them for earthquake resistance. The following figures illustrate some of the applications of PFDs in real life.



**Figure 2.12** Improving the seismic resistance of the boeing commercial airplane factory by PFDs, everett, washington, USA (Pall and Pall, 2004).



**Figure 2.13** Moscone west convention center equipped with PFDs, San Francisco, USA (Pall and Pall, 2004).



**Figure 2.14** Providing PFDs for the Cafeteria and Auditorium Buildings in Boeing Development Center, Boeing Field, Seattle, WA, USA (Pall and Pall, 2004).

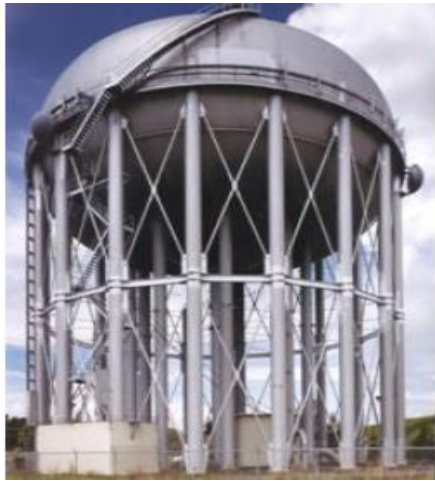


**Figure 2.15** The use of PFDs in Provincial Police Headquarters in Quebec, Montreal, Canada (Pall and Pall, 2004).



**Figure 2.16** Three-Million Gallon Reservoir equipped with PFDs, Sacramento, California, USA (Pall and Pall, 2004).



**Figure 2.17** Concordia University Library Building with the addition of PFDs, Montreal, Canada (Pall and Pall, 2004).



**Figure 2.18** A view of Sharp Memorial Hospital's ambulatory care center with PFDs, San Diego, California, USAResponse (Pall and Pall, 2004).



**Figure 2.19** General View of St. Joseph medical center patient tower with PFDs (Shao et al., 2006).

#### 2.1.4: Rotational Friction Damper RFD

According to Mualla and Belev's suggested damping device in 2002 (Figure 2.20), which consists of a middle steel plate, two side plates, and two friction pad discs circular in shape positioned in-between the steel plates, RFDs are made up of these components. On a single-story frame built with RFD, they carried out experimental and numerical analyses. In a framed structure supported by RFD, the middle (central) plate is connected to the girder midspan by a hinge. As illustrated in Figure 2.21, the four ends of the two side plates are attached to the inverted V-brace elements. Pretensioned bars are used in the bracing system to prevent compression stresses and buckling. The damper device and the column bases are pin-connected to the bracing bars at both ends. Combining two side plates with one center plate expands the frictional surface area and offers the symmetry which is necessary to achieve the device's planar action. The three damper plates are joined by a pre-tightened bolt. The role of this adjustable bolt is to control the compression force transmitted to the interfaces of the steel plates and friction pad discs.

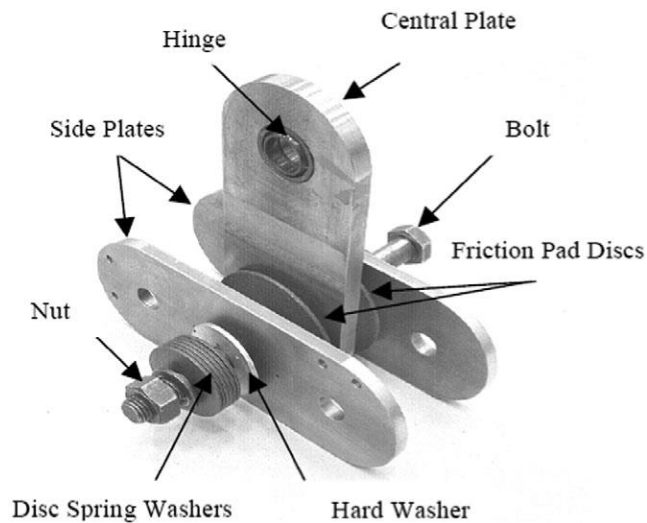


**Figure 2.20** Details of the RFD device suggested by Mualla and Belev (Mualla and Belev, 2002).

The frame system tends to move horizontally when a lateral force stimulates it. The bracing system and the friction forces generated at the intersection of the friction pads and steel plates will counteract the horizontal motion. The operation of the RFD device



under lateral excitation is shown also in Figure 2.21. The cables connected to the damper device are only subjected to tensile forces. The device is pretty simple in its construction, and it may be set up in a variety of bracing arrangements to provide a full and effective damping system.

A building or structure can resist a strong seismic event if the earthquake's energy input is less than the capacity of the structure or building to absorb energy. Through the displacements and deformations of structural elements, which comprise damping energy, elastic strain energy, kinetic energy, and inelastic hysteretic energy, the input energy of a seismic motion communicated to a structure can be dissipated. Once an RFD is installed in a structure, the RFD can minimize the structural damage brought on by the accumulated hysteretic energy by converting a portion of the earthquake's input energy into damping or dissipated energy (H. Jarrahi, 2020).

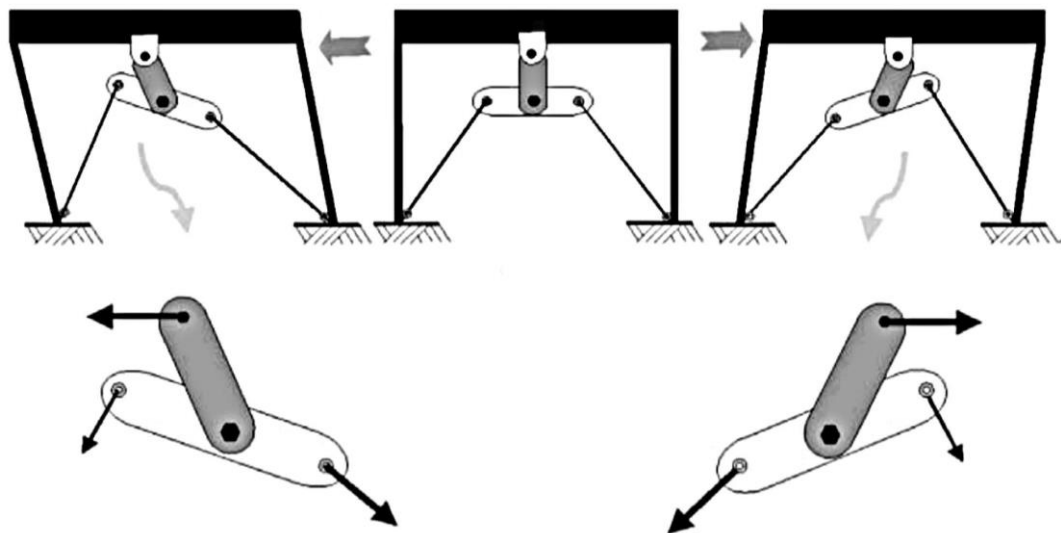


**Figure 2.21** The RFD's operating system (Mualla and Belev, 2002).

### 2.3 Friction Damped Braced Frames FDBF

Each brace in FDBFs is connected by a friction joint that will slide at a certain shear force value and this force is predetermined. Friction damped braces are not expected to move under the influence of wind forces or small seismic events, but they will move and dissipate energy during a strong earthquake while still providing a constant resisting force. As the MRF comes into operation, the building's shear resistance increases. Up to the initial yield, this increasing resistance of the frame is linear. Serious damage to the structure has not been done up to this point because the frame is still in the elastic region. FDBs may disperse the most seismic energy by optimizing the stiffness and slip force of the brace. Any yielding of the frame offers different ways to dissipate energy, providing a degree of security that is not available by alternative framing schemes. Modeling the actual performance of friction devices during earthquakes is important to get the behavior of the FDBF systems.

The basic hysteretic behavior of any friction joint that slides in tension and compression in FDBF system is represented in Figure 2.22. It indicates that the friction brace's force-displacement relation is linear before the force exceeds the slip force,  $P_s$ . The brace then slides with regular slip force, dissipating the seismic energy through the sliding joint, and acting as a damper. After the maximum displacement has been released, the hysteretic loop moves to a direction parallel to the original elastic branch, where it remains until slip of the friction joint starts in the opposite direction.

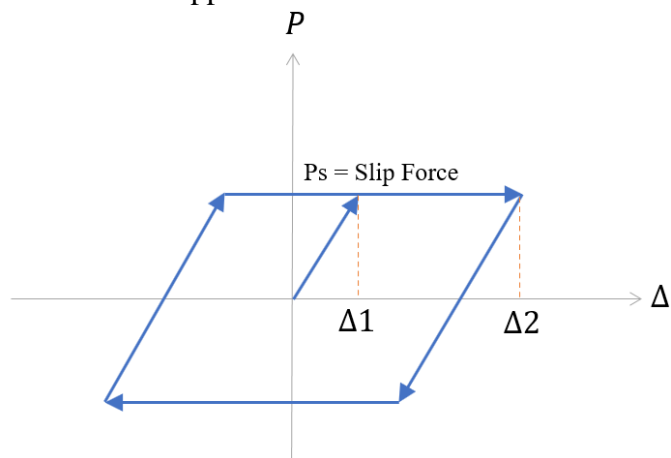


**Figure 2.22** Hysteretic behavior of a friction damped steel brace.

The FDBF performs consistently and repeatably, and their hysteresis loops are rectangular with minimal fading across several more reversals cycles than are experienced in successive seismic events. Friction has a much larger capacity for extracting energy than any technique that requires the damping process of material yielding. Buildings that vibrate may be made to slow down their motion by braking rather than breaking, much like cars.

Each brace added to the MRF to form the FDBF structural system, is equipped with a friction device. When there are strong seismic events, the device slips at a certain load before the frame's other structural components start to yield. The device's slippage then offers a mechanism for the loss of energy by friction. The braces will face a constant load, and the MRF will absorb the remaining loads. In this way, forces are redistributed across entire stories, causing all the bracing to slip and take part in the energy dissipation process. The following properties are combined in such a modified structural system (Pall and Cedric Marsh, 1982):

- Under service load situations, such as wind and small earthquakes, it acts like a braced frame structure and has enough stiffness to limit deflections.
- The device's flexibility rises as a result of the device's tendency to slip during big earthquake excitations, which results in extended oscillation periods and, as a result, generally reduced invitation to seismic loads.
- It delays or prevents the yielding of important structural components by dissipating a significant amount of energy by friction during slippage.

#### **Braces with Friction Device in FDBF system.**

As long as the brace is designed to not buckle in compression case up to the value of slip load, a friction joint having slotted holes can be employed to slide in both tension and compression. Before the brace buckles, friction joints that slide under high tension and low compression loads are also acceptable. Most frequently, the bracing system is slender and intended to be effective only under tension. In this situation, the friction joint slips under tension loads but will not slip back in the reversal of load. The brace offers

relatively little energy dissipation in the succeeding cycle since it won't slide until it has been stretched past its previously extended length.

In any arrangement of the bracing system, friction devices may be utilized. Friction joints can be advantageously employed to link curtain walls or preassembled infill panels to the frame, which function as bracing components. Additionally, the system may easily be added to already existing framed buildings to improve their earthquake protection.

### **Optimum Slip Load of Friction Damped Braces**

The value of energy input and energy output determines a structure's seismic response. Therefore, limiting the gap between input energy and energy loss results in the optimum seismic response. The input energy essentially depends on the structure's natural period and the dynamic properties of the ground motion. By adjusting the dynamic properties of the structure in relation to the forcing motion, it may be controlled to some extent. This is actually workable in ground movements with narrow band properties. Control of the input energy alone is unreliable because future ground motion characteristics are very unpredictable in nature and connected with uncertainties caused by soil structure interaction. However, the period of the FDBF changes with the amplitude of the oscillations, or the magnitude of the seismic motion, and is controlled by the slip load of the brace. The resonance of the structural system is consequently more complex to establish.

The slip load and slip movement during each excursion are proportional to energy loss in the braces. The energy dissipation by friction will be negligible for a very high slip load since there won't be any slip. Again, the quantity of energy dissipation will be minimal if the slip load is much low. There is a midpoint between these two extremes that will provide the most energy dissipation. Depending on how the slippage of the bracing softens the structure with respect to the frequency of the ground motion, this may invite more or less seismic forces. The favorable impacts of energy dissipation must be paired with the potential positive or negative consequences of the changing period of vibration on the energy intake. Therefore, the reaction of the structure may be "tuned" to an ideal value by making the right slip load selection.

## 2.4: Previous Studies and Research

**Pall and Marsh (1982)**, an analysis of the FDBF system's response was performed by Pall and Marsh. Dynamic analysis was obtained to analyze three different types of 10-story frames, including moment resisting frame, moment resisting frame with braces, and FDBF, under the assumption that all structures would face the same earthquake ground motion. The comparisons were based on top roof displacements and responses of their time-history, maximum moments value in the beams, the maximum shear envelope of all columns, and structural damage. It was demonstrated that the bracing system in the frames significantly increased the seismic resistance of FDBF while causing no material yielding.

**Andre Filiatrault (1988)**, An innovative and effective modeling methodology for the seismic design and analysis of steel structures using a novel friction damping system was presented in this work. The theoretically derived hysteretic characteristics of the friction devices were included in the FDBF Analysis Program, which can be used in a microcomputer system. The building of a design slip load spectrum results from a parametric analysis of single-story FDBF system using the Program. A straightforward design equation and design slip load spectrum have been created using this model in a parametric study for a quick and accurate assessment of the optimum slip load of single-story friction-damped buildings. The ground motion predicted at the building site is taken into consideration in the design equation, together with the characteristics of the structure.

**Baktash, (1989)**, provided a study on the FDBF system which include three different arrangements, K-braced, Z-braced, and X-braced frames were investigated. In order to disperse the most energy possible using FDBs, the concept of optimizing the slip load of the brace was established. Nonlinear dynamic analysis was also performed to compare the FDBF and standard frames without a damping device and the comparisons were given in tables and charts. A steel model of the FDBF was created and placed to the test on a shaking table during that examination. For all types of Friction damped bracing systems, the floor displacements, elemental forces, and structural damage were much less than for frames without dampers.

**Dowdell and Cherry (1996)**, suggested two semi-active schemes: the Semi-Active Friction Damper and the other one is "off-on" friction damper. The slip force was alternately regarded in the "off-on" system between zero and a predefined constant value, but in the other system, it was continually taken into account in response to the structure's state of deformation. It was shown that these two systems might greatly improve a passive friction-damped structure's performance. The use of the FDBF was expanded from symmetric frames to unsymmetric frames by redistributing the slip load of the friction devices throughout the plan layout of the structure.

**C. Adam (1999)**, Numerical research was performed on the dynamic response of earthquake-excited FDBFs with secondary structures. Several elastic and inelastic structural characteristics were taken into account. Examples of single-degree-of-freedom oscillators mounted to four-story frame structures with a range of structural characteristics were studied in a parametric investigation. The dynamic response of four distinct primary structures is contrasted: First, an elastic-plastic shear structure with friction braces, secondly, an unlimited elastic braced shear structure without slipping, third structure was an unlimited elastic frictional damped braced shear structure, and finally an elastic-plastic shear structure without braces. The El Centro earthquake sample's north-south strong motion component was used as a test seismic input, and investigations were conducted at various levels of strong-motion seismic events. Comparisons are made between decoupled and coupled oscillator responses. While decoupling findings are demonstrated to be relatively accurate for detuned frequencies, the peak response at tuned frequencies is significantly overestimated.

**Er Mao Gong (2004)**, The goal of this investigation was to employ the Modal Pushover Analysis (MPA) method to estimate the performance of Friction Damped Braced Frame (FDBF) systems as well as to validate its accuracy by comparing it with FEMA-273 Pushover Analysis procedure and Nonlinear Response History Analysis (NL-RHA). An Improved Modal Pushover Analysis (IMPA) was also applied to address the shortcomings of the MPA procedure. Two types of moment resistant steel frame structures were chosen in the study, the first one is a single-story steel frame, while the

second structure was multi-story. In order to expand the application of pushover analysis to multi-degree-of-freedom systems from single-degree-of-freedom systems. For both structural systems, FDBs were added to evaluate their performance characteristics during the seismic event. When IMPA and NL-RHA findings are compared, the errors are markedly smaller than those of the MPA approach, particularly for determining the story drifts. It is found that the IMPA technique is more preferable than FEMA-273 pushover analysis in calculating the floor displacement, the story drift, and the plastic slip of the FDBs by comparing the seismic demands values with those obtained from NL-RHA.

**Luis Altamira (2009)**, performed a study on seismic inter-story drift demands for three different friction damped braced structures. Three types of framing structures were selected, 3, 9, and 20-story structures. The behavior of FDBFs has been thoroughly studied utilizing current trends, codes, and assessment standards. Other studies' findings about the efficiency of FDBFs were proved. Results of the analysis revealed that the incorporation of the FDBs resulted in average decreases in the peak inter-story drift ratios of roughly 70% for the 3-story structure, 62% for the 9-story structure, and 35% for the 20-story structure. Additionally, collapse of the buildings was frequently prevented in addition to the inter-story drifts being greatly decreased and brought to acceptable levels. According to the study, limiting or preventing residual/permanent inter-story drifts should be taken into consideration while determining the devices' optimum frictional force.

**Felix C. Blebo (2013)**, Results from research work indicate that local yielding of the member may happen at the base of the first story outer columns in self-centering, concentrically braced frame (CBF) as a result of the concentrated vertical load applied on a single self-centering CBF column under rocking. In order to solve this problem, Blebo developed a self-centering FDBF that limits structural damage and residual drift while offering large nonlinear drift capability without uplift and pounding of the column. Beams, columns, and braces that branch out of a central column make up the FDBF system. Beams, columns, and braces that branch out of a central column make up the FDBF system. Friction in the lateral-load bearings between the FDBF system at each floor and the gravity system is employed to dissipate energy, much like the self-

centering CBF. Post-tensioning bars with a vertical orientation offer more overturning moment resistance and minimize residual drift.

**Felix C. Blebo (2015)**, This time Blebo studied the FDBF system with buckling restrained columns (BRC), which was created to reduce damage and residual drift with no column uplift and to give a large drift capacity. In order to reduce the total seismic response for the FDBF-BRC system, energy is dissipated through the BRCs and friction is produced at the lateral-load bearings. The FDBF-BRC system's behavior and seismic response were examined using nonlinear static and dynamic evaluations of nine prototype structures to assess the impact of the frame strength factor and BRC strength factor. Increasing BRC strength lowers the framing weight and the ratio of Post-tensioning bar yield force to yield force of BRC, according to comparisons of the design parameters. The technology can prevent soft story collapse and decrease structural damage during earthquakes, according to dynamic and nonlinear static pushover studies. Increasing the BRC strength improves the system's ability to dissipate energy, which lowers the story drift responses and peak roof drift. This initial investigation reveals that the self-centering FDBF-BRC could be a significant lateral force resisting system, providing more system ductility than traditional CBF systems without column uplift of old investigated SC-CBF systems.



### 3. MATERIALS and METHODS

This section will explain the details of the structural systems evaluated within the scope of the thesis and the methods used. The moment resisting frames were taken from the thesis (Arat 2020). Then, diagonal braces as well as friction-damped braces were added to each story to improve the seismic performance.

In this investigation, The main objective is to compare the seismic performance of selected framing systems (Moment Resisting Frame MRF, Braced Frame BF, and Friction Damped Braced Frame FDBF). The frames represents the behavior of two steel structures with 4-bay, 4-story for the first system and 5-bay, 9-story for the second system. The two-dimensional external frames of these structures were chosen to make the required comparison. The structures were designed by the deformation based design approach. Static and dynamic performance analyses of the structures were conducted.

#### 3.1 Building Model

##### 3.1.1 System Description

Within the scope of this thesis, two different multi-story buildings were examined. Geometric features such as the number of floors, heights, and floor areas of these buildings are given in Table 3.1 in detail. Figure 3.1 shows the floor plan and front view of our 4-story building. In Figure 3.2, the plans of the 9-story structure are given.

**Table 3.1.** Geometric properties of the selected structures

Number of Floors	Floor Range	Floor Height (m)	Floor Area (m <sup>2</sup> )
4 Floors	1-4	4	54*36= 1944
9 Floors	1	5.4	45*45= 2025
	2-9	4	

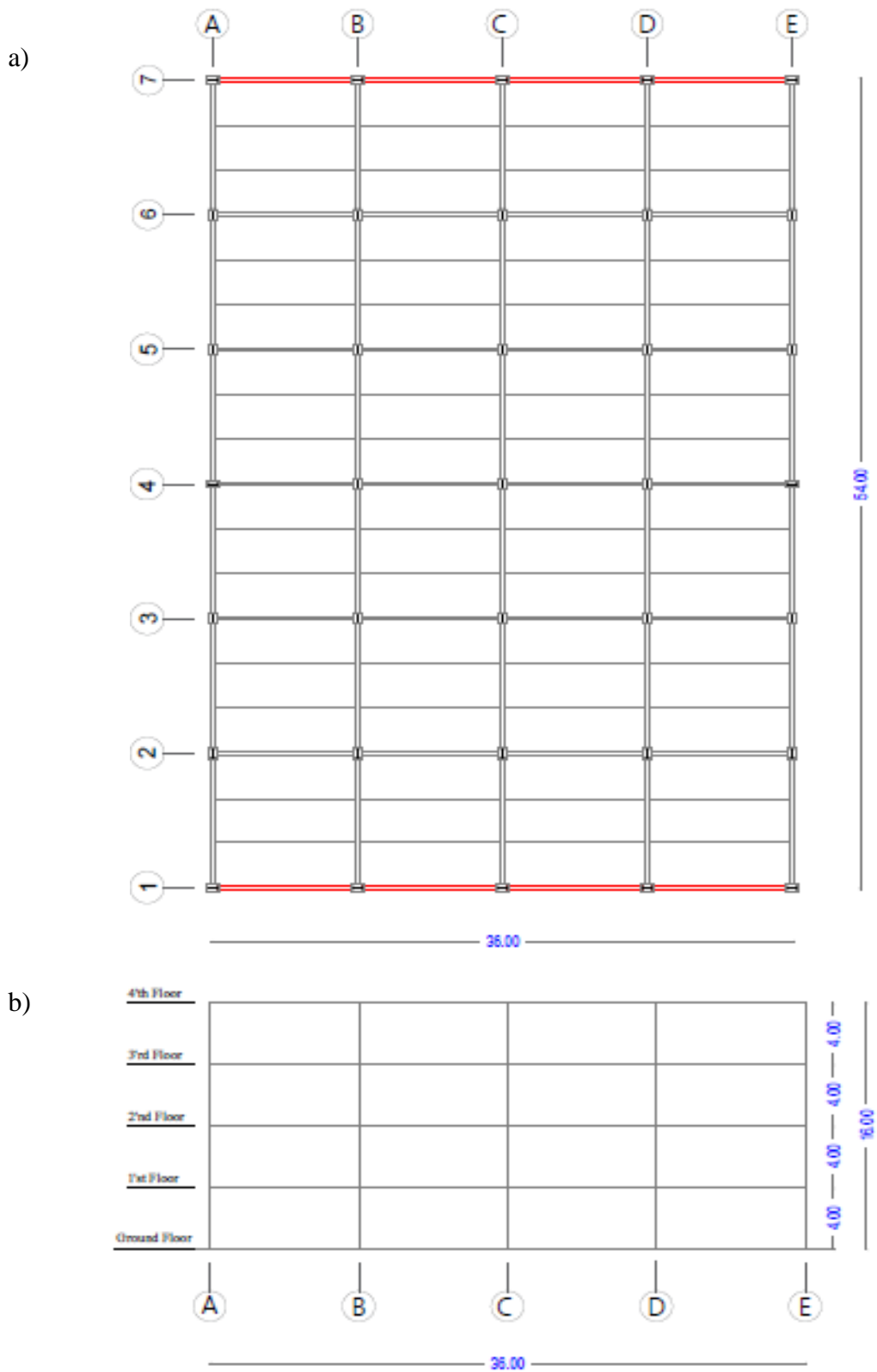


**Figure 3.1** The 4-story steel structure. **a)** Plan view **b)** side view and floor heights

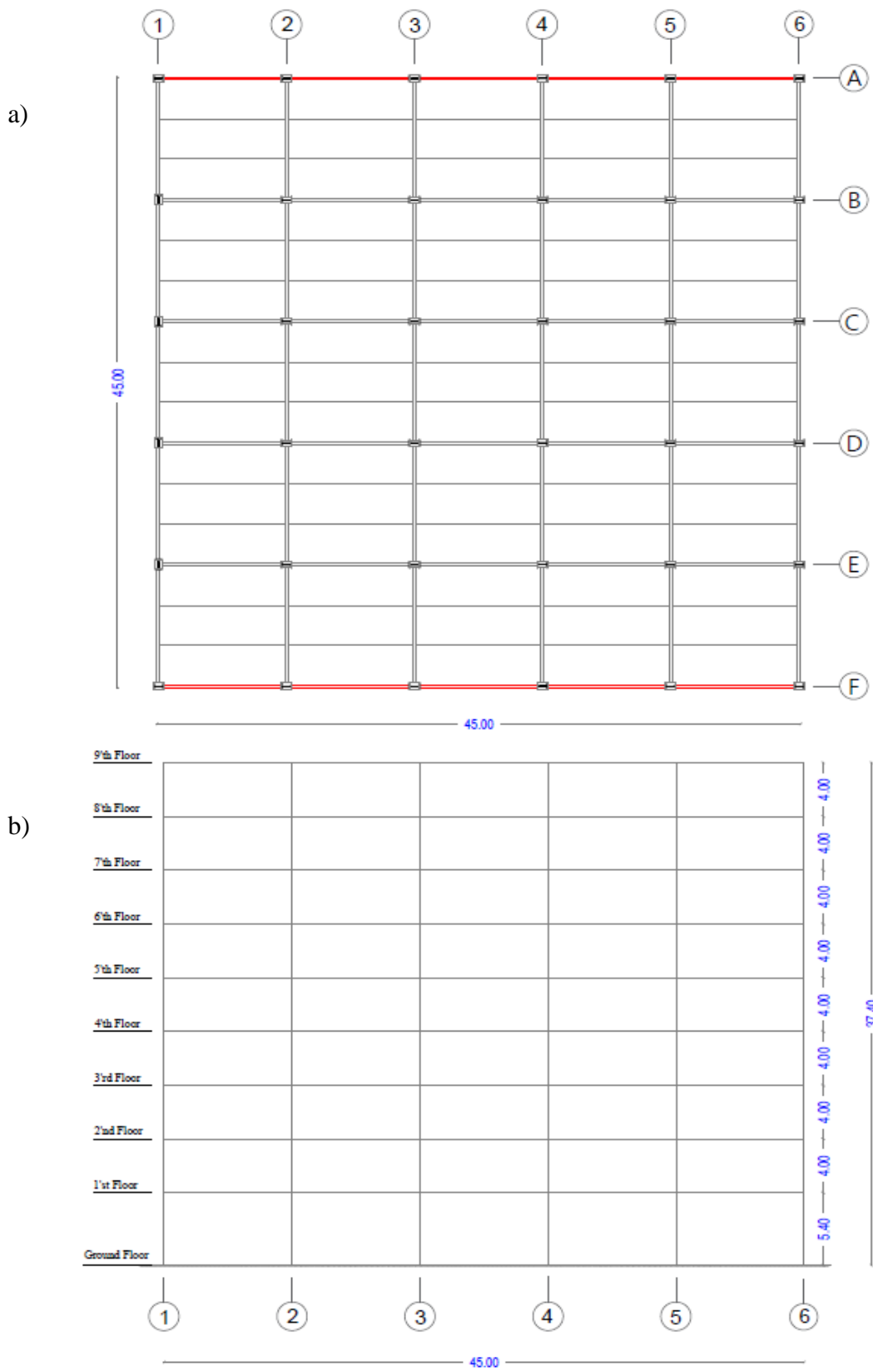


**Figure-3.2** The 9-story steel structure. **a)** Plan view **b)** side view and floor heights

ASTM A992 Grade 50 is used as the material in all steel frame systems. Information about this material is given in Table 3.2.

**Table 3.2.** ASTM A991 Grade 50 material properties

$F_y$ (MPa)	$F_u$ (MPa)	$E$ (MPa)	$F_{ye}$ (MPa)	$F_{ue}$ (MPa)
345	450	200000	379.5	495

### 3.1.2 Loads applied on systems

The load conditions of the 4- and 9-story buildings within the scope of this thesis were taken directly from the sources. The value of loads acting on the external MRF of the structure were calculated in the thesis of Arat (Arat 2020), and values were taken directly from there. These loads are given in Table 3.3. The distributed and single loads that these area loads act on beams and columns are given in Tables 3.4 and 3.5. For example, in the 4-story building shown in Figure 3.3., the loads are shown in Table 3.6. The same way for the 9-story system calculates the values.

**Table 3.3.** Loads acting on the buildings

Place	Type	Load (kN/m <sup>2</sup> )
<b>Roof</b>	Steel material	0.3
	Dead Load (G)	4.3
	Live Load (Q <sub>r</sub> )	1
<b>Normal Floor</b>	Steel material	0.3
	Dead Load (G)	5.3
	Live Load (Q)	3.0

**Table 3.4.** Distributed load acting on beams

Story	G	Q
	Dead Load(kN/m)	Live Load (kN/m)
Roof	6.45	1.5
other	7.95	6.0

**Table 3.5.** Normal load acting on columns

Story	G		Q	
	Dead Load (kN)		Live Load (kN)	
	Inner Column	Outer Column	Inner Column	Outer Column
Roof	116.1	58	27	13.5
Other	143.1	71.55	108	54

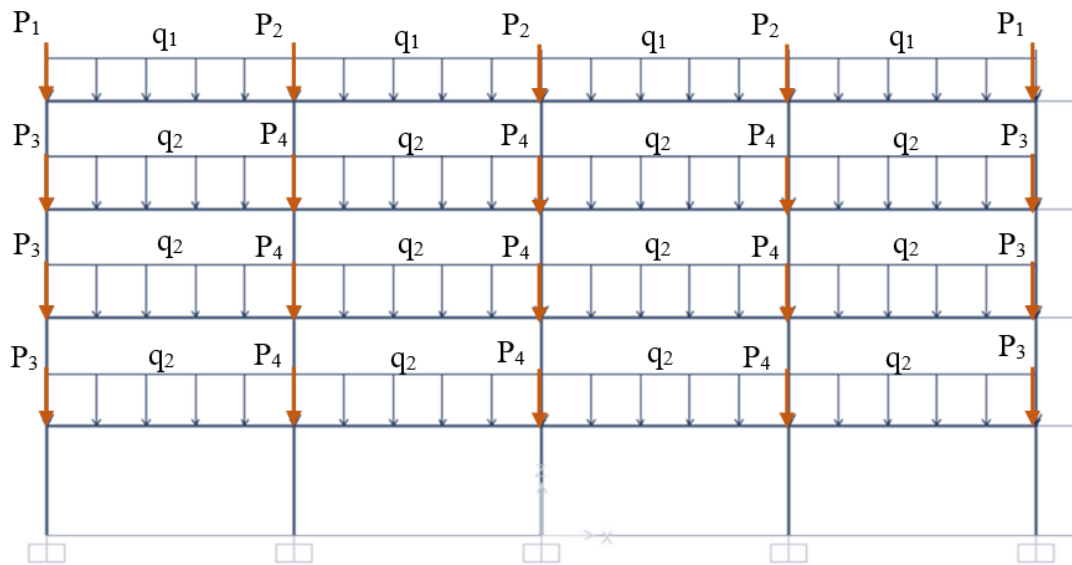


**Figure 3.3.** Vertical loads acting on the MRF in a 4-storey system

**Table 3.6.** Values of vertical loads acting on 4 story MRF

<b>Name of the Load</b>	<b>Value</b>	<b>Unit</b>
q <sub>1</sub>	10.02	kN/m
q <sub>2</sub>	13.6	kN/m
P <sub>1</sub>	90.122	KN
P <sub>2</sub>	180.39	KN
P <sub>3</sub>	122.38	KN
P <sub>4</sub>	244.76	KN

### 3.1.3. Earthquake parameters

The necessary earthquake parameters related to the structures within the scope of the thesis were determined according to Turkish Seismic Code for Buildings (TSCB 2018). The calculated earthquake parameters are given in Table 3.7. The parameters used in these calculations were taken from Arat's thesis (Arat 2020).

**Table 3.7.** Earthquake parameters

<b>Parameters</b>	<b>Value</b>
Building Significance Factor	1
Ground Class	ZB
$S_s$	1.58
$S_1$	0.82
$F_s$	0.9
$F_1$	0.8
$S_{DS}$	1.422
$S_{D1}$	0.656
$T_A$	0.093
$T_B$	0.46
Earthquake Design Class	1
Earthquake Level to be Used	DD-2

The details of the lateral design spectrum calculation according to TSCB are shown in Figure 3.4.

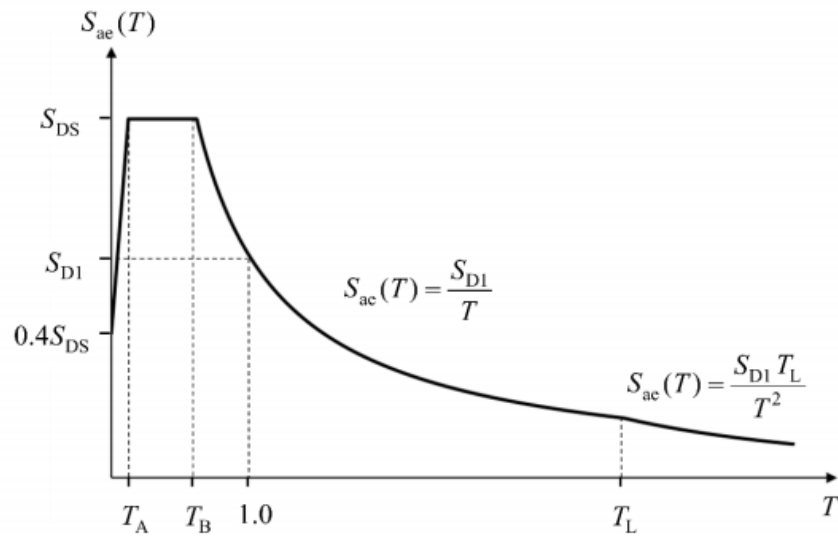


**Figure 3.4.** Lateral elastic design response spectrum (TSCB 2018)

### 3.2. Nonlinear modelling and analysis

This section gives nonlinear materials and analysis methods of the models to be compared. Plastic hinge definitions were made using the concentrated plasticity method. Plastic hinges are defined to comply with ASCE 41-13 regulation. Nonlinear static analysis and nonlinear dynamic analysis methods in time history are shown.

#### 3.2.1. Modeling of Plastic Hinge

In Figure 3.5, the generalized force-deformation relationship for steel elements is given. a,b,c,A,B,C,D,E values were obtained from FEMA-356. The axial force-moment relationship for the elements under axial load is given in Equation 3.1 and Equation 3.2. In SAP2000, hinges specify how an element behaves nonlinearly. As the hinge approaches the region of the force-displacement curve that is negatively sloped, its

capacity decreases. When the hinge comes to the level where noticeable strength deterioration starts, the software raises the base shear value, and if the increased base shear causes an increase in lateral displacement, the program continues the same process. If the increase in base shear value does increase in lateral displacement, the software decreases the base shear value till the force within the hinge becomes constant. The generalized force-displacement curve in Figure 3.5 illustrates this process.

All members unload as the base shear decreases, which also results in a reduction in the lateral displacement. Once the hinge has been entirely unloaded, the base shear as well as lateral displacement increases once more, and the other structural members take on the load that the unloaded hinge had been carrying.

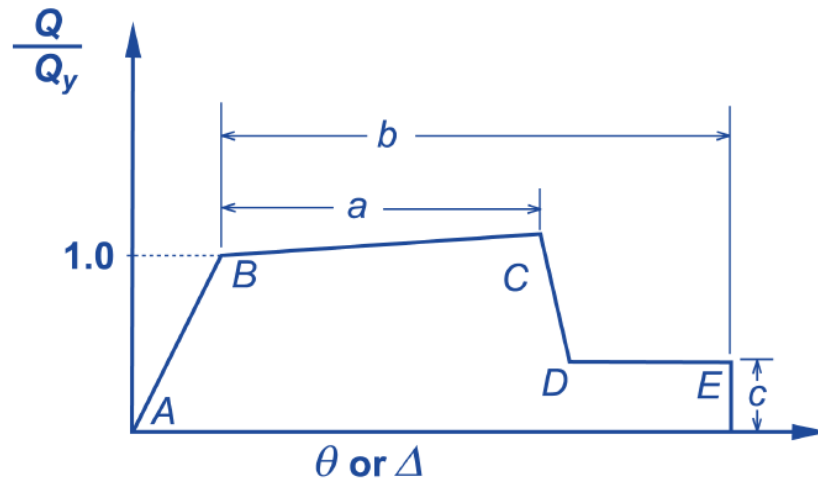


**Figure 3.5.** Generalized Force Displacement Curve (FEMA 356).

$$\frac{P}{P_y} + \frac{8 M_{pc}}{9 M_p} = 1 \quad \frac{P}{P_y} \geq 0.2 \quad (3.1)$$

$$\frac{P}{2P_y} + \frac{M_{pc}}{M_p} = 1 \quad \frac{P}{P_y} < 0.2 \quad (3.2)$$



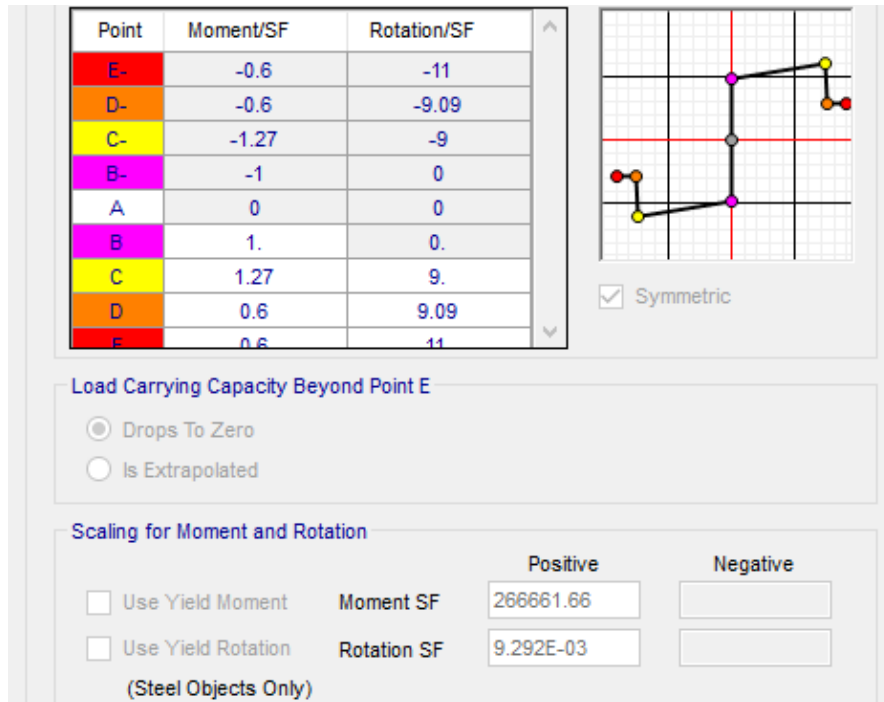


**Figure 3.6.** Moment-rotation relationship of HE700A element in Sap 2000.

In Figure 3.6, the properties of the plastic hinge of HE700A section assigned using the Sap 2000 program are given. Axial force-moment relations are given in Figure 3.7, moment-rotation relations in Figure 3.8 and Figure 3.9.

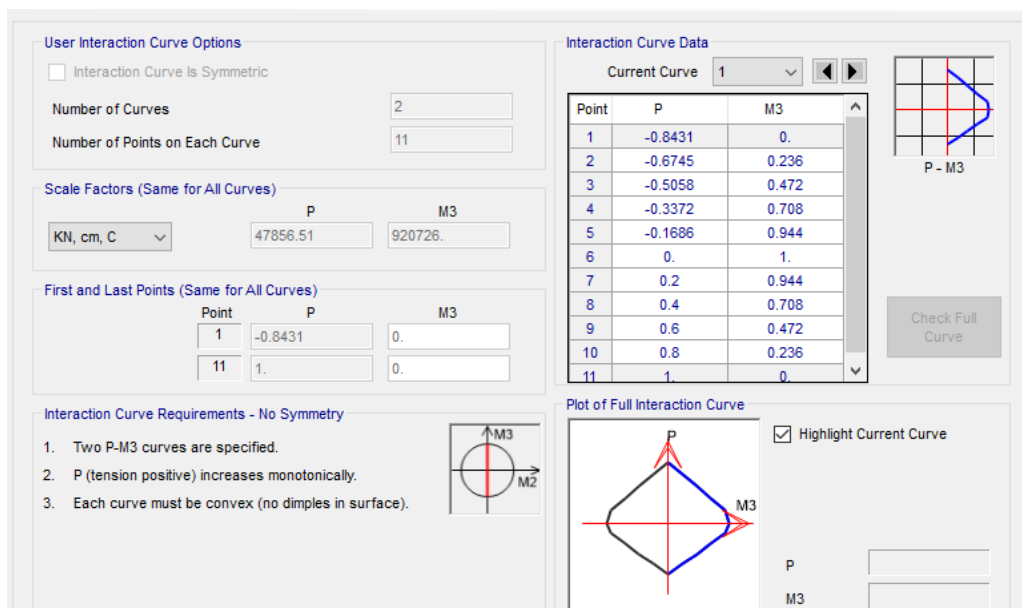


**Figure 3.7.** Axial force-moment relationship in Sap 2000 program.

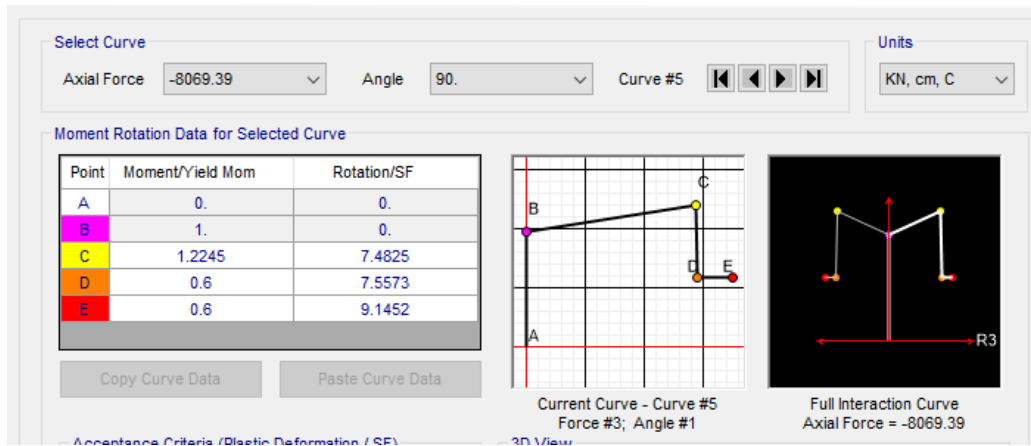


**Figure 3.8.** Moment-rotation relationship at 20% axial force capacity level in Sap 2000 program.

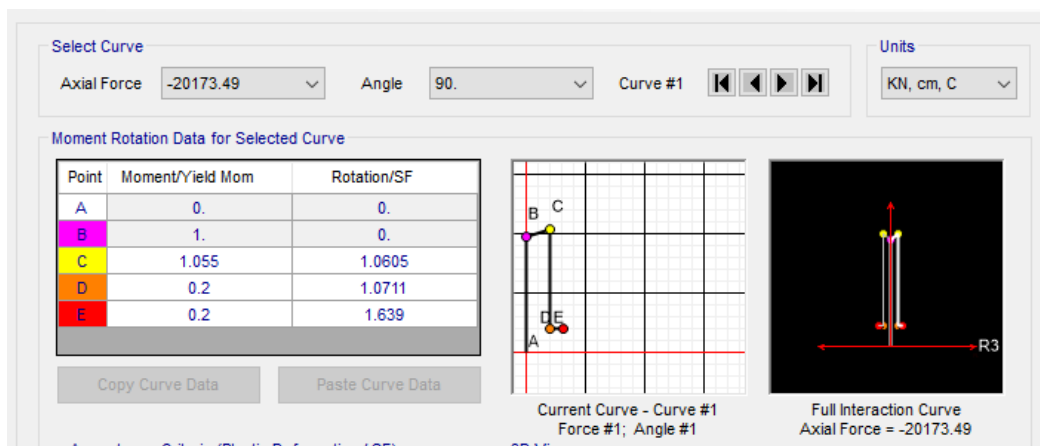


**Figure 3.9.** Moment-rotation relationship at 80% axial force capacity in Sap 2000 program.

### 3.2.2 Nonlinear static (pushover) analysis

Nonlinear static analysis or what is known as Pushover analysis, is a simplified method for predicting deformations of the structure. As the main components of a building yield or fail during an earthquake, the dynamic forces applied to the building are transferred to other structural components and thus the building begins to redesign itself to absorb the seismic forces. The pushover theory can be simulated via structural analysis software by applying lateral loads distributed along the building height until the weak joint is found in the building or until a target displacement is reached. The model is then revised to take into consideration new structural changes caused by the weak joint. The loads are distributed again through the second iteration. Lateral loads are applied again to Push the structure until the second weak joint is located. This process continues over and over until the yield pattern of the entire structure is determined under seismic forces when it gets into a target displacement. The capacity curve is obtained after performing nonlinear static analysis which represents the relation between base shear in the vertical axis and displacement in the horizontal axis. The maximum value of the base shear is determined at the top displacement of the structure. Figure.3.10 illustrates the principle of this method.

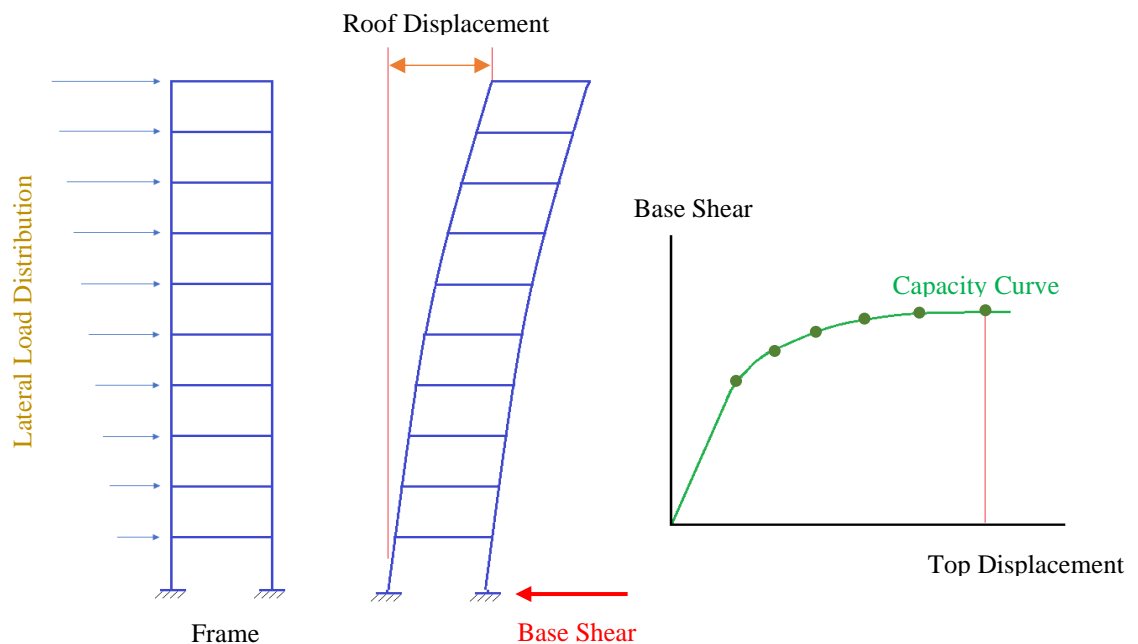


**Figure 3.10.** Nonlinear static (Pushover) analysis method.

Pushover analysis is known as a nonlinear static method since the applied action is static, while the structural behavior is nonlinear. It is a relatively simple solution for complex structures to evaluate seismic behavior in terms of predicting deformation and force values, which requires the application of severe ground motion to structures and their elements in nonlinear analysis.

There are several things taken into consideration during the analysis. Pushover analysis assumes that structures oscillate mostly in the lower modes of vibrations during seismic motion, in which the structure of a Multi-degree-of-freedom MDOF system is simplified to an equivalent single-degree-of-freedom SDOF system. It means that the seismic response of the system is controlled by the first vibration mode only. This analysis method aims to detect crack sequence in the system, plastic hinge formation, yielding, and failures.

### **General Steps of Pushover Analysis**

The researcher can execute pushover analysis using specialized and customized codes by performing the subsequent steps:

- a) The overall structural system behavior is described by a two- or three-dimensional software model.
- b) The load-deformation diagrams are defined in bilinear or trilinear shape of all main components that affect lateral response.
- c) The structural model or system is first subjected to gravity loads made up of dead loads and a certain portion of live loads.
- d) Then, a lateral load pattern that is pre-defined and dispersed along the structure height is applied.
- e) Increases in lateral loads are made until one or more members start to yield under the combination of lateral load effect and gravity effect.
- f) At the initial yielding, the values of base shear and roof displacement are observed and recorded.

- g) The structural model is adjusted to take into consideration the components' decreased stiffness.
- h) In order to let other members yield in the redesigned structural model, gravity loads are eliminated and a new lateral load increment is applied. It should be noted that the updated structural model is subjected to a new individual analysis with zero starting conditions for every incremental lateral load. As a result, member forces are calculated at the end of an incrementally lateral load analysis by combining the forces from the most recent analysis to the total of the forces from the prior increments.
- i) The base shear and roof displacement accumulation values are obtained by adding the roof displacement and lateral load increments to the corresponding preceding total values.
- j) Till the roof deformation reaches a specific degree or the system becomes unstable, steps (g), (h), and (i) are replicated.
- k) To get the pushover curve or global capacity curve of the structure, the roof displacement value corresponding to the base shear value is plotted as seen in Figure 3.11.

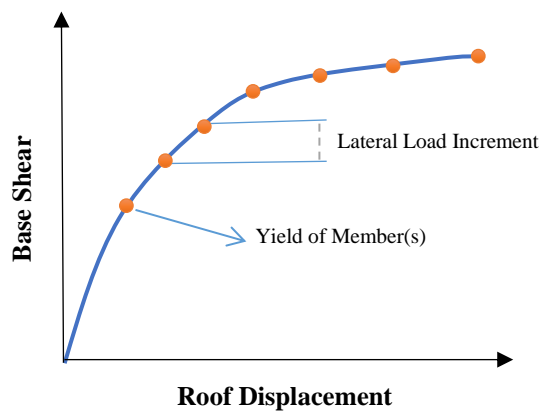


**Figure 3.11.** Global Capacity Curve of The Structure (Pushover Curve).

Equation 3.3 was used as the load combination for vertical loading, which is the initial step of the static pushover analysis. However, the non-linear vertical loading combination prepared in the Sap 2000 program is given in Figure 3.14. In this combination, the vertical earthquake effect  $E_d^{(Z)}$  was calculated according to Equation 3.4. (TSCB)

$$G + Q_e + 0.2S + E_d^{(H)} + 0.3E_d^{(Z)} \quad (3.3)$$

$$E_d^{(Z)} = (2/3)S_{DS}G \quad (3.4)$$

The state of the structure loaded according to Figure 3.14 was used as the initial step of the pushover analysis. In these settings, the lateral load distribution is automatically assigned by the Sap 2000 program according to TSCB 2018.

P-Delta column was added to the system in order to include the second order effects in the model. The P-Delta column included in the system is shown in Figure 3.12. The column here does not have any lateral stiffness. The equivalent earthquake load calculation of Sap2000 program according to TSCB 2018 is shown in Figure 3.13.

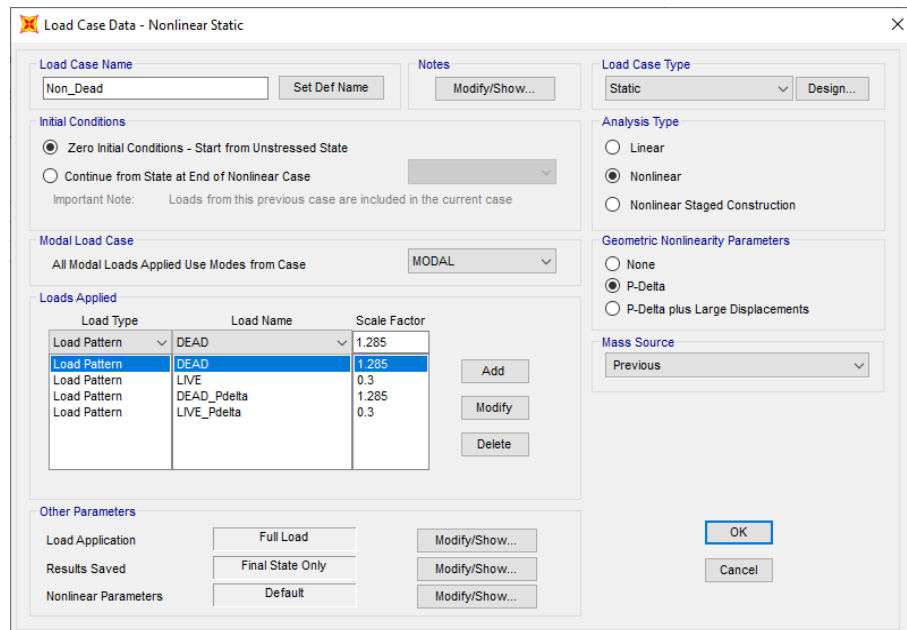


**Figure 3.12.** Non-linear vertical loading combination.

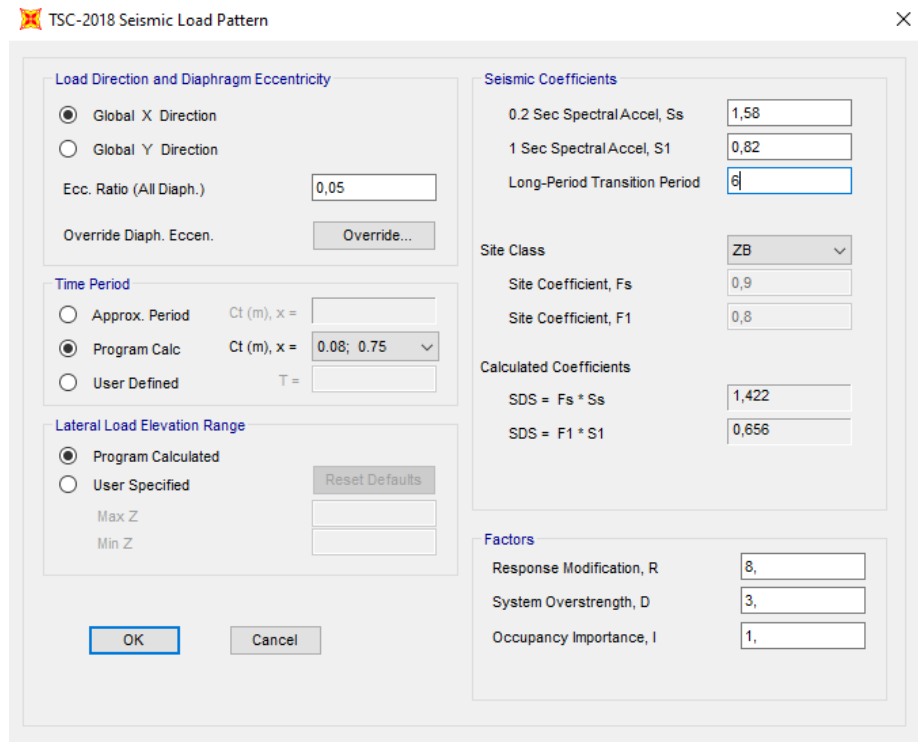


**Figure 3.13.** Equivalent earthquake load calculation of Sap2000 program according to TSCB 2018.

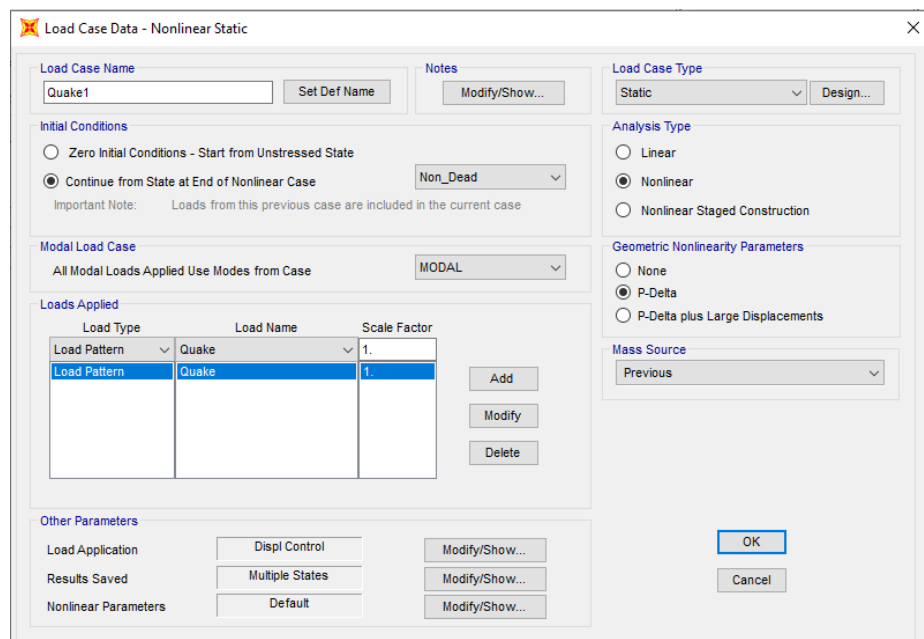


**Figure 3.14.** Parameters of Pushover analysis of the structure in Sap2000 program.

As a result of the analysis applied, the values of the peak displacement-base shear force of the capacity were obtained for the structure.

### 3.2.3 Time history analysis

The time-history analysis is a nonlinear dynamic analysis technique to determine the structural dynamic response under a specific load that may vary over time. It is important for seismic analysis of structures as it provides the most realistic dynamic load specifications. In this study, time history analysis was carried out using the finite element analysis software SAP2000. In order to use this method, appropriate earthquake records are required first. In the selection of these records, earthquake magnitudes, fault distances, source mechanisms, and local ground conditions will be taken into account. These earthquake records were taken from PEER databases (TSCB), and they are described in Table 3.8 and Table 3.9 for 4 and 9 story frames respectively.

**Table 3.8.** Earthquake records selected for the 4-story structure

<b>Ground motion No.</b>	<b>Name of the earthquake</b>	<b>Station</b>	<b>Intensity</b>
<b>983</b>	Northridge-01	Jensen Filter Plant Generator Building	6.69
<b>1013</b>	Northridge-01	LA Dam	6.69
<b>8164</b>	Duzce_ Turkey	IRIGM 487	7.14



**Table 3.9.** Earthquake records selected for the 9-story structure

<b>Ground motion No.</b>	<b>Name of the earthquake</b>	<b>Station</b>	<b>Intensity</b>
<b>983</b>	Northridge-01	Jensen Filter Plant Generator Building	6.69
<b>1111</b>	Kobe_ Japan	Nishi-Akashi	6.9
<b>4456</b>	Montenegro_ Yugoslavia	Petrovac - Hotel Olivia	7.1

### **3.3 Slip Load and Stiffness of the FDBs**

The load at which the damper begins to slip during seismic occurrences is known as the slip load of friction damper or FDB. The friction damping systems are made to be stable against wind loads. However, they slide during a big earthquake before the yielding of structural elements. There are several approaches to design the optimum slip load in order to maximize the dissipation of seismic energy. The approach proposed by [Baktash, 1989] will be followed in this investigation. Baktash found that when the shear resisted by the damped brace  $V_b$  is equivalent to that of the frame without bracing  $V_f$ , the friction damped bracing system dissipates the most energy.

$$V_b = V_f \quad (3.5)$$

The shear resisted by the multi-story system, in the FDBF for weak beam/strong column equals.

$$V_b = V_f = n * \frac{2 M_{pb}}{h} \quad (3.6)$$

$M_{pb}$  : the yield moment of the beam.

h: the height of each floor

n: the number of bays in the frame

The geometric relationship shows that the braces' slip load,  $P_s$ , is

$$P_s = \frac{V_f}{\cos \varphi} = n * \frac{2 M_{pb}}{h \cos \varphi} \quad (3.7)$$

$\varphi$  : The angle at each floor between the beam and the brace.

Moving to the stiffness of the braces, to check the stiffness of the brace, the optimum stiffness ratio between the brace and the frame should be  $\lambda=4$  to 5. Following dynamic analysis using sap2000 program, the stiffness of FDBF and MRF is compared as follows.

$$\frac{K_{FDBF}}{K_{MRF}} = \frac{\omega_F^2}{\omega_M^2} \quad (3.8)$$

$K_{FDBF}$  is the stiffness of FDBF,  $K_{MRF}$  is the stiffness of MRF,  $\omega_F$  is the first natural frequency of FDBF.  $\omega_M$  is the first natural frequency of MRF. The stiffness ratio between the brace and the frame can be calculated using the following equation.

$$\lambda = \frac{K_b}{K_f} \quad (3.9)$$

The slip load values as well as sections of braces are shown in next chapter (section 4.2). The slip load of FDB can be defined to plastic hinge properties of the element in sap2000 program. As an example, figures 3.15 and 3.16 show the definition of slip loads for the braces in first floor in 4-story and 9-story systems respectively.

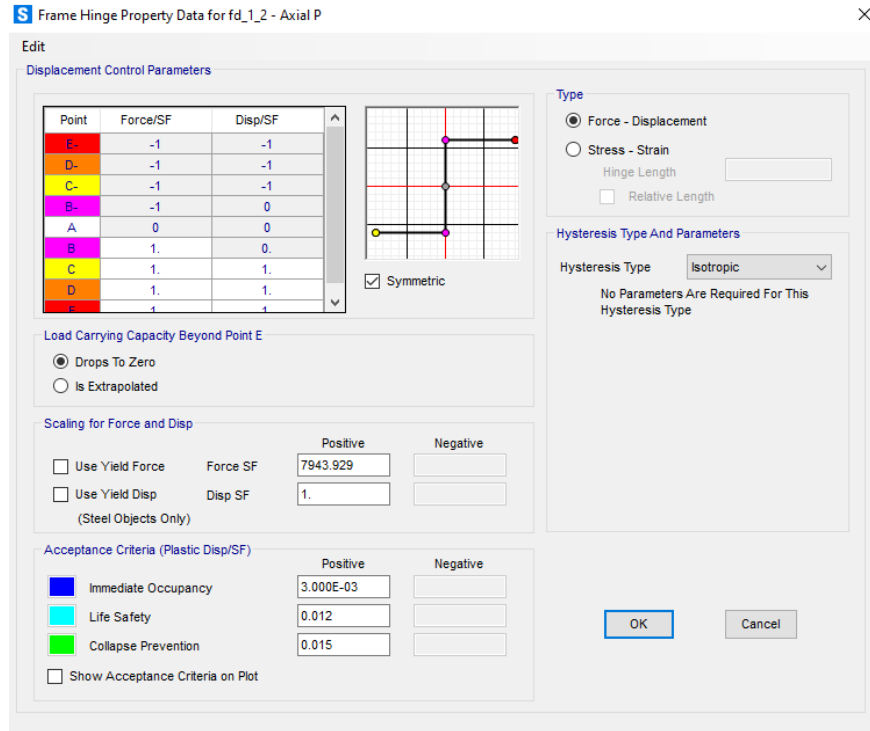


Figure 3.15. Plastic hinge properties of FDB in first floor of 4-story FDBF system.

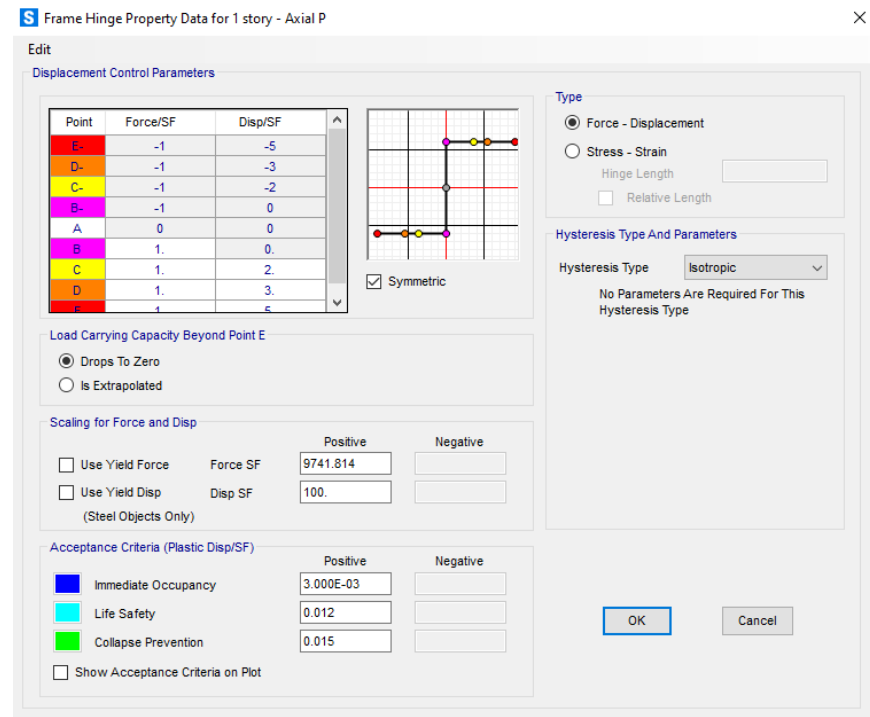


Figure 3.16. Plastic hinge properties of FDB in first floor of 9-story FDBF system.

## 4. RESULTS AND DISCUSSION

In this chapter, the description and discussion of the results obtained from both chosen analysis methods (time history analysis and pushover analysis), which were applied to 4- and 9-story frame systems will be given. The Four-bay four-story MRF system and The Nine-bay five-story MRF system are equipped one time with diagonal braces and another time with FDBs. In this chapter, a comparison between these three framing systems will be provided. In the graphs that contain all framing systems and included in this chapter, the BLUE curves represent the behavior of MRF, Red curves for BF, and the ORANGE curves represent the behavior of FDBF.

### 4.1. Period and Frequency values

Table 4.1 shows the comparison of the period and frequency values for all frames for the first three modes of 4-story systems, while Table 4.2. shows the comparison of the period and frequency values of 9-story systems. It can be noticed that the period values of the structure oscillations has been shifted to a lower value due to adding friction dampers to the system. The reduction is equal to 60% in the period for the first mode in 4-story FDBF and about 52% for the first mode in 9-story FDBF, while for the other modes the reduction is also considerable. The reduction means an increase in frame stiffness which reduces the effect of vibration on the structural and nonstructural components.

**Table 4.1.** Values of period and frequency for first three modes of 4- story MRF, BF, and FDBF

Mode	Period Sec			Frequency Cyc/sec		
	MRF	BF	FDBF	MRF	BF	FDBF
1	1.045212	0.414515	0.414515	0.956744	2.4124579	2.41245789
2	0.296313	0.135887	0.135887	3.374815	7.3590446	7.3590446
3	0.13897	0.077082	0.077082	7.195781	12.973277	12.9732769

**Table 4.2.** Values of period and frequency for first three modes of 9- story MRF, BF, and FDBF

Mode	Period Sec			Frequency Cyc/sec		
	MRF	BF	FDBF	MRF	BF	FDBF
1	2.217016	1.073983	1.073983	0.451057	0.931113	0.931113
2	0.784639	0.318434	0.318434	1.274472	3.140372	3.140372
3	0.435148	0.167978	0.167978	2.29807	5.953167	5.953167

#### 4.2. Slip load and stiffness of braces

By recalling the equation (3.7) presented in chapter 3, the slip load of FDBs can be calculated and defined in plastic hinge properties of the brace in sap2000 program. Also, stiffnesses of the braces can be checked by using the way explained in chapter 3 and by substituting in equation (3.8) after the selection of cross sections of braces. Table 4.3 shows the values of slip loads as well as sections selected for 4-story systems, and Table 4.4 shows these values of 9-story braced and friction damped braced frames. Knowing that 10% has been added to the slip forces as an assumption to consider the effect of vertical forces applied on the system.

**Table 4.3.** Values of slip forces and brace sections for 4-story systems

STORY	$M_{pb}$ (KN.m)	h(m)	No. of Bays	slope of FDB	Brace Section	$P_s$ (KN)
4	2666.61	4	4	24	H400X551	6421.729703
3	2666.61			24	H400X551	6421.729703
2	3298.7			24	H400X593	7943.928722
1	3298.7			24	H400X593	7943.928722

**Table 4.4.** Values of slip forces and brace sections for 9-story systems

<b>STORY</b>	<b>M<sub>pb</sub>(KN.m)</b>	<b>h(m)</b>	<b>No. of Bays</b>	<b>slope of FDB</b>	<b>Brace Section</b>	<b>Friction Force (KN)</b>
9	2028.72	4	5	24	H400X463	6106.953905
8	2028.72	4		24	H400X463	6106.953905
7	2666.61	4		24	H400X634	8027.162128
6	2666.61	4		24	H400X634	8027.162128
5	3298.76	4		24	H400X818	9930.091518
4	3298.76	4		24	H400X818	9930.091518
3	3298.76	4		24	H400X818	9930.091518
2	4099.27	4		24	H400X990	12339.82656
1	4099.27	5.4		31	H400X990	9741.814472

### 4.3 Comparison of Top Displacements

Starting with time history analysis by conducting the selected ground motions, the maximum value of roof displacement for 4-story MRF under RSN 983 ground motion is 224.53 mm, 103.01 mm for BF, and 51.85 mm only for FDBF which forms a reduction in 54% comparing with MRF after the addition of diagonal braces and about 77% after the addition of FDBs in FDBF system. Moving to 9-story frames, the roof displacement of MRF under RSN 983 ground motion is 549.89 mm, 262.19 mm for BF, and 230.89 mm for FDBF and this forms a reduction in 52% for BF system and about 58% for FDBF. Table 4.5 shows the top displacement values of all frames under selected ground motions. The comparison of roof displacements of 4-story frames under different ground motions is illustrated in Figure 4.1, and Figure 4.2 for 9-story systems.

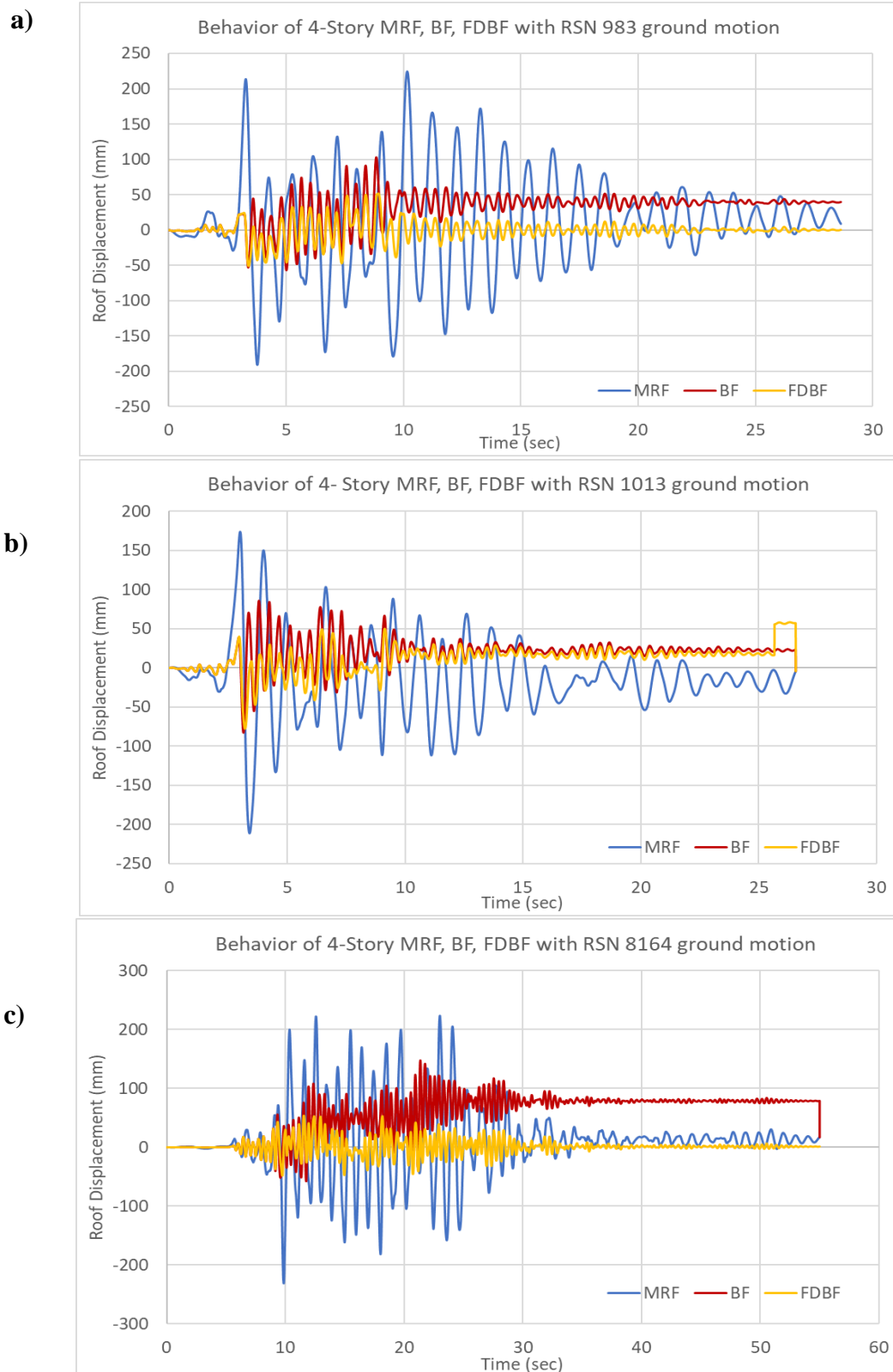


**Figure 4.1.** Comparison of roof displacements of 4-story frames under different ground motions. a) RSN 983 b) RSN 1013 c) RSN 8164

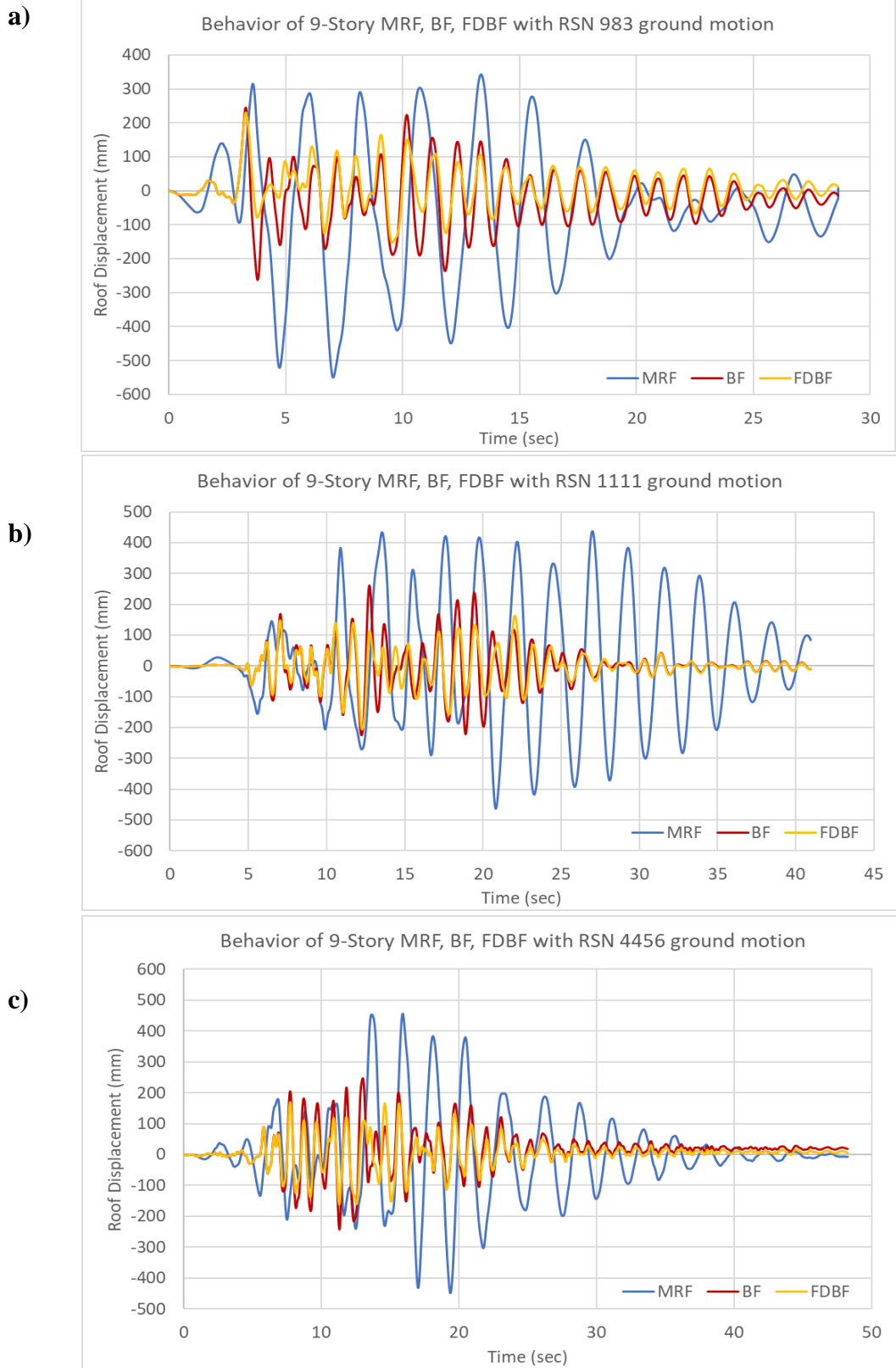


**Figure 4.2.** Comparison of roof displacements of 9-story frames under different ground motions a) RSN 983 b) RSN 1111 c) RSN 4456



**Table 4.5.** Values of top displacements for all systems

Top displacement values in (mm) for 4-Story systems								
MRF			BF			FDBF		
RSN 983	RSN 1013	RSN 8164	RSN 983	RSN 1013	RSN 8164	RSN 983	RSN 1013	RSN 8164
224.53	211.28	231.31	103.01	85.67	147.5	51.85	77.74	53.6
Top displacement values in (mm) for 9-Story systems								
MRF			BF			FDBF		
RSN 983	RSN 1111	RSN 4456	RSN 983	RSN 1111	RSN 4456	RSN 983	RSN 1111	RSN 4456
549.89	463.08	455.94	262.19	261.14	246.96	230.89	205.49	169.58

#### 4.4 Comparison of Relative Story Drifts

In order to evaluate the 4- and 9-story frames selected within the scope of this thesis, the value of relative story drifts were compared. The maximum relative story drift values obtained under different ground motions are given in Figure 4.3 and Figure 4.4 for the 4 and 9 story frames respectively. The average relative story drift values are given in Figure 4.5 for all frames.

The Figures showed that the FDBF system can control the story drifts significantly compared to the first and second systems (MRF and BF). The maximum relative story drift value for 4-story system was about 1.5% in MRF, 0.9% for BF, and 0.6% for FDBF which forms a reduction in about 60% comparing with results obtained from MRF analysis. For 9-story frames, the maximum relative story drift value was about 1.8% in MRF in fourth story, 1.0% in BF in ninth story, and 0.7% in FDBF system in the first story. This gives a reduction of relative story drift in 9-story FDBF in about 60% also compared with MRF. As can be seen, the values of FDBF obtained are homogeneously spread from the lower story to the upper story.

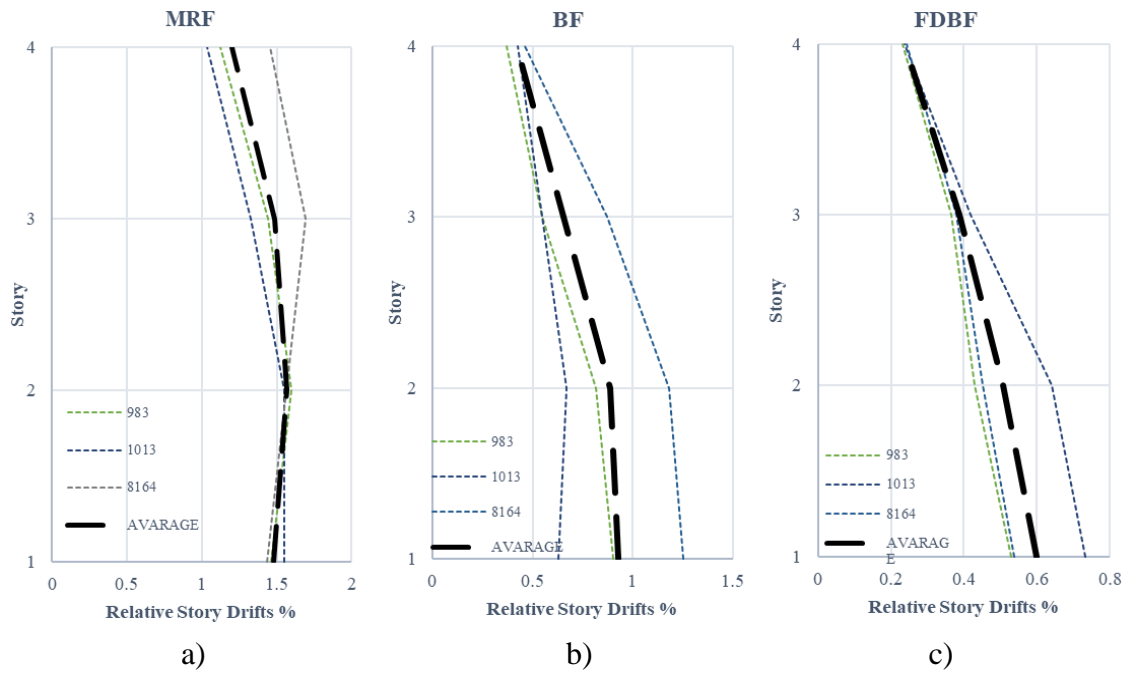


**Figure 4.3.** Comparison of relative story drift ratios of 4-story frames under different ground motions. a) MRF b) BF c) FDBF

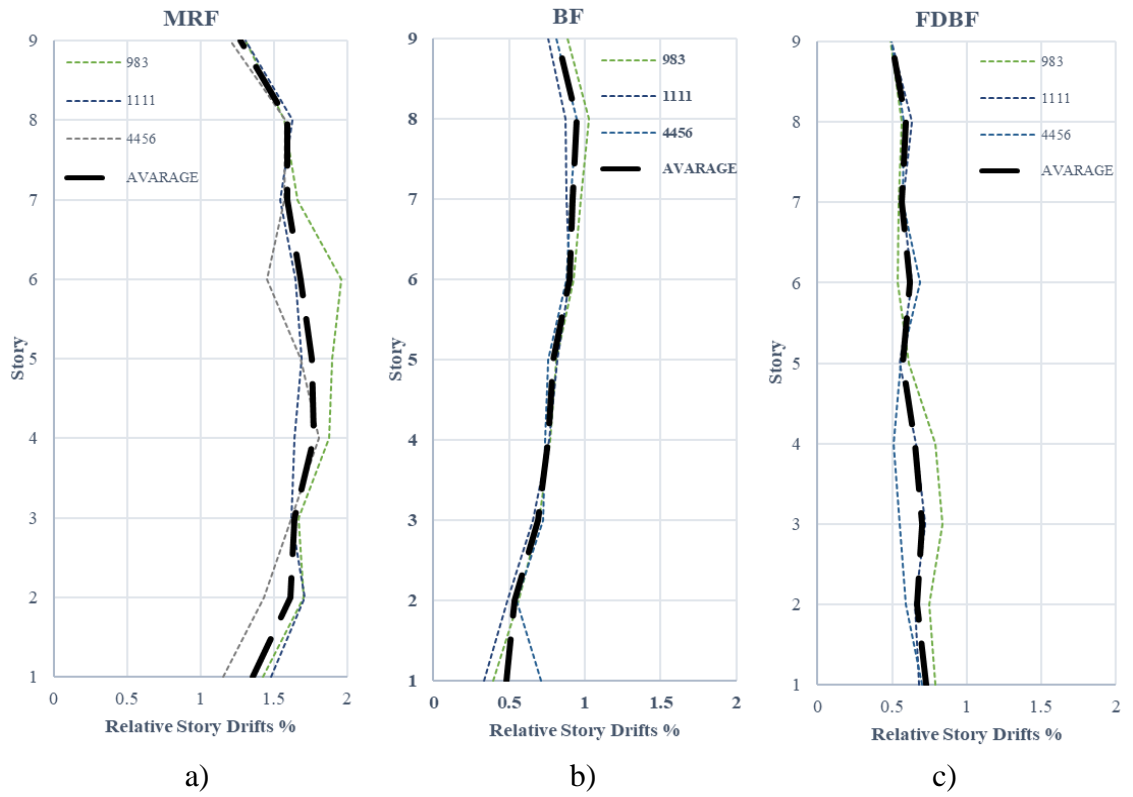


**Figure 4.4.** Comparison of relative story drift ratios of 9-story frames under different ground motions a) MRF b) BF c) FDBF

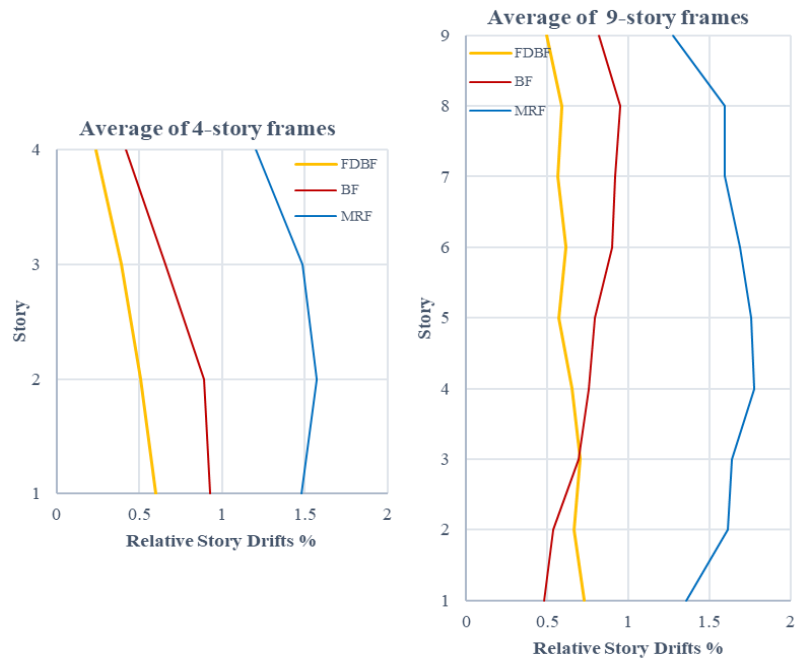


**Figure 4.5.** Comparison of average values of relative story drifts % under different ground motions for all frames. **a)** 4-story frames **b)** 9-story frames.

#### 4.5 Comparison of Shear Forces

In Figure 4.6, and Figure 4.7 story shear forces obtained for 4- and 9-story systems are given, after the application of selected ground motions (RSN 983, RSN 1013, and RSN 8164 for 4-story systems & RSN 983, RSN 1111 and RSN 4456 for 9-story systems). As can be seen, the shear force values in the structure with FDBs increased less than the BF structure compared with MRF. The comparison of average values for all frames can be seen in Figure-4.8, which shows that the maximum shear force in 4-story MRF is 10501 KN, 24677 KN for BF, and 14118 KN for FDBF. For 9-story systems, the maximum shear force in MRF equal to 11970 KN, 28865 KN for BF, and 16767 KN for FDBF. When comparing all systems, it can be noticed that the maximum shear force of 4-story FDBF increased by 35% comparing with MRF, while the maximum shear force of BF increased by 135% . For 9-story, the maximum shear force of FDBF increased by 40% comparing with MRF, while the maximum shear force of BF increased by 141%. It also appears from the graphs that the shear forces decrease more regularly as we go up to higher floors in the FDBF systems.

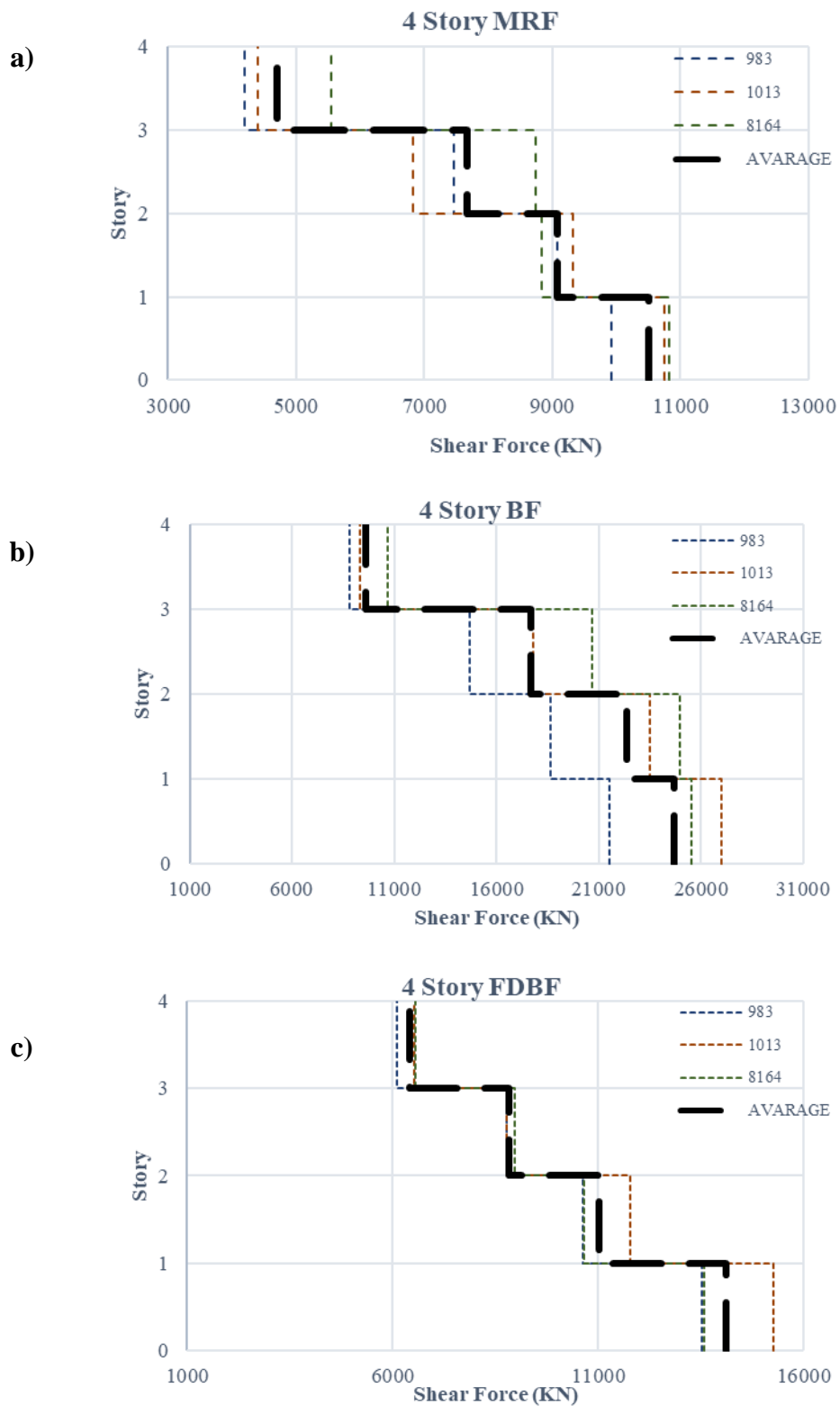


**Figure 4.6.** Comparison of shear force values under different ground motions applied on 4-story frames. a) MRF b) BF c) FDBF

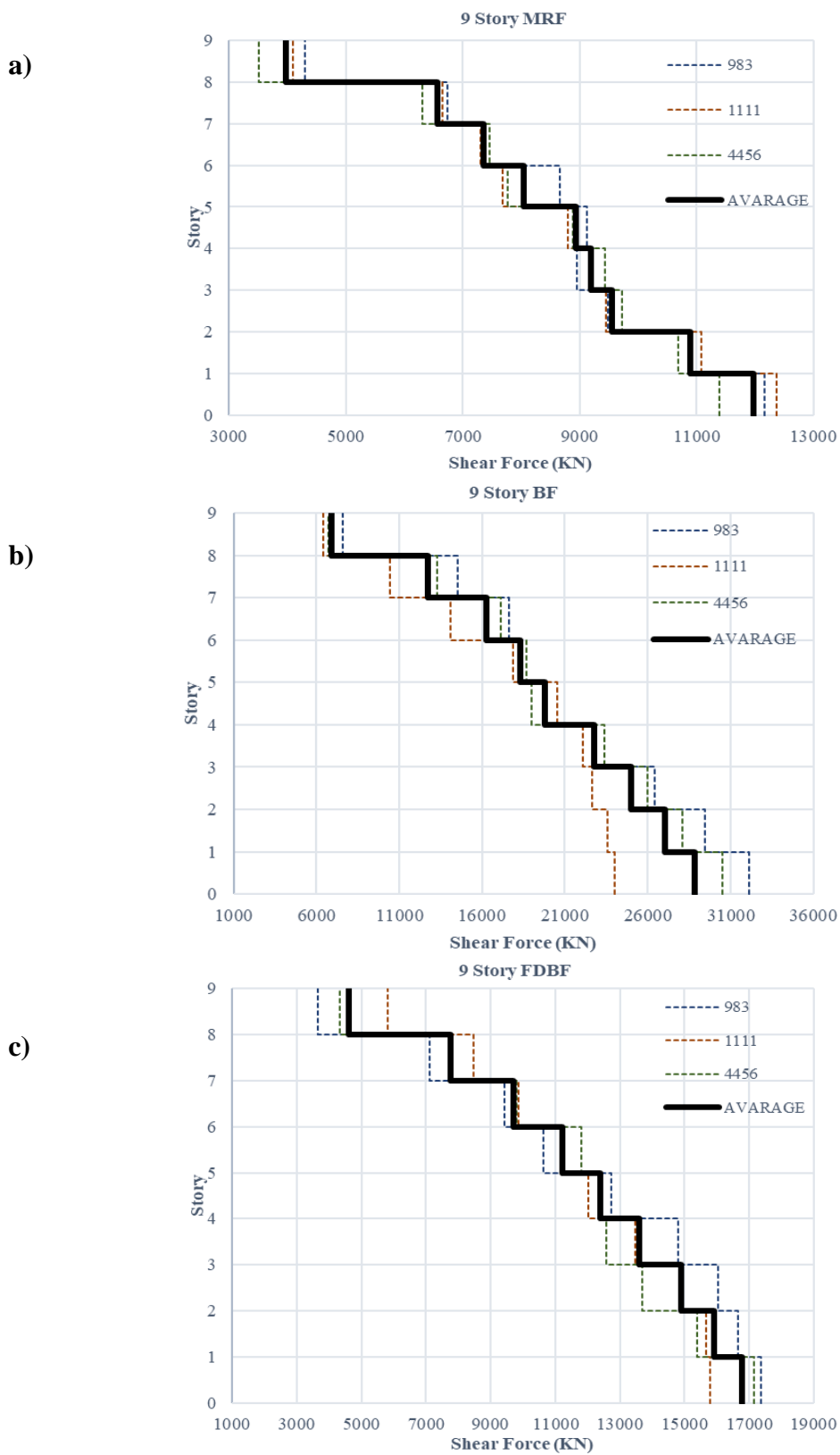


**Figure 4.7.** Comparison of shear force values under different ground motions applied on 9-story frames. a) MRF b) BF c) FDBF

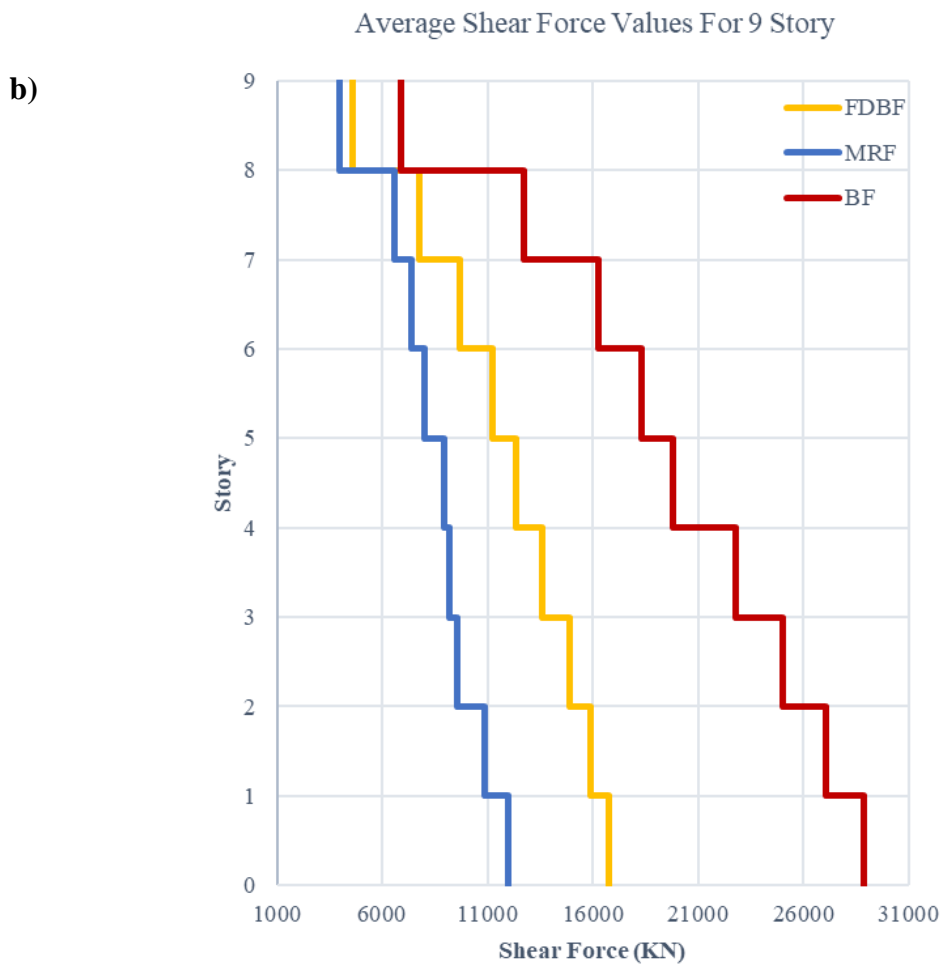
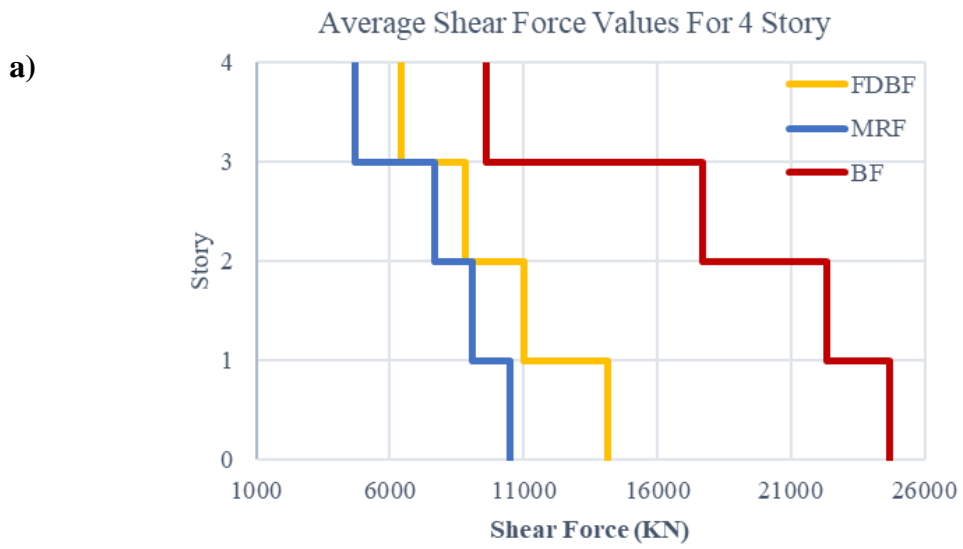


**Figure 4.8.** Comparison of average values of shear forces under different ground motions for all frames. a) 4-story frames b) 9-story frames.

#### 4.6 Pushover (Capacity) Curves

Another method of analysis was applied on all systems selected in this investigation which is the static nonlinear (pushover) analysis. The base shear forces for all systems were compared as seen in Figure- 4.9 (a) for four-story systems, and Figure-4.9 (b) for nine-story systems.

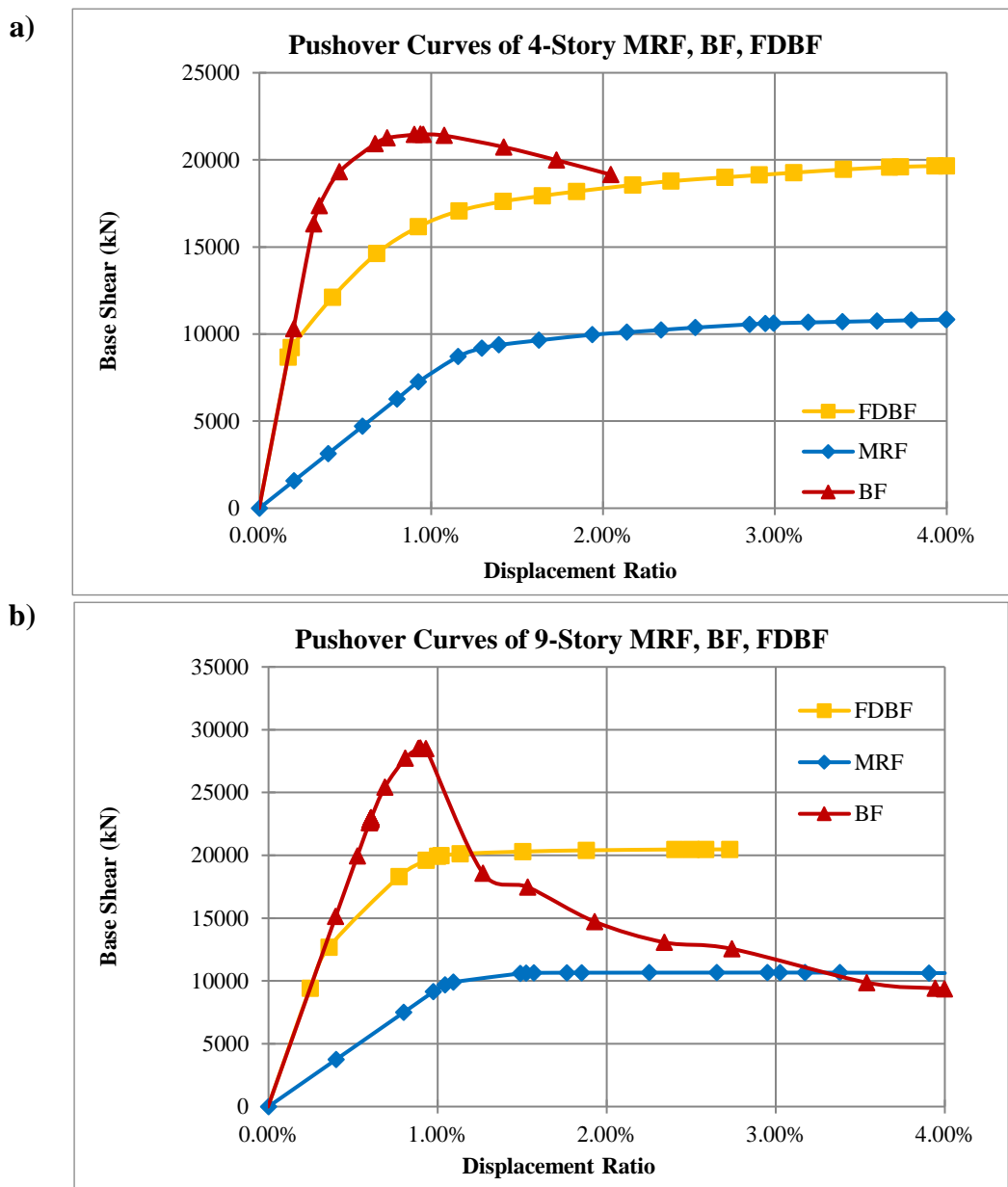


**Figure 4.9.** Comparison between pushover curves (capacity curves) for all frames  
a) 4- Story frames b) 9-Story frames

## 4.7 Plastic Hinges State

The plastic hinges state as a result of applying different ground motions in time history analysis can be seen in this section. Figures 4.10, 4.11, and 4.12 show the state of plastic hinges under RSN 983, RSN 1013, and RSN 8164 respectively for 4-story systems, while Figures 4.13, 4.14, and 4.15 show the plastic hinges under RSN 983, RSN 1111, and RSN 4456 respectively for 9-story systems. By adding FDBs, beams and columns are protected from yielding and hinge formation. It is noted that there are no plastic hinges formed in the main element of FDBF system. and what we see in the figures is only a showing of the sliding movement of the friction dampers due to ground motion.

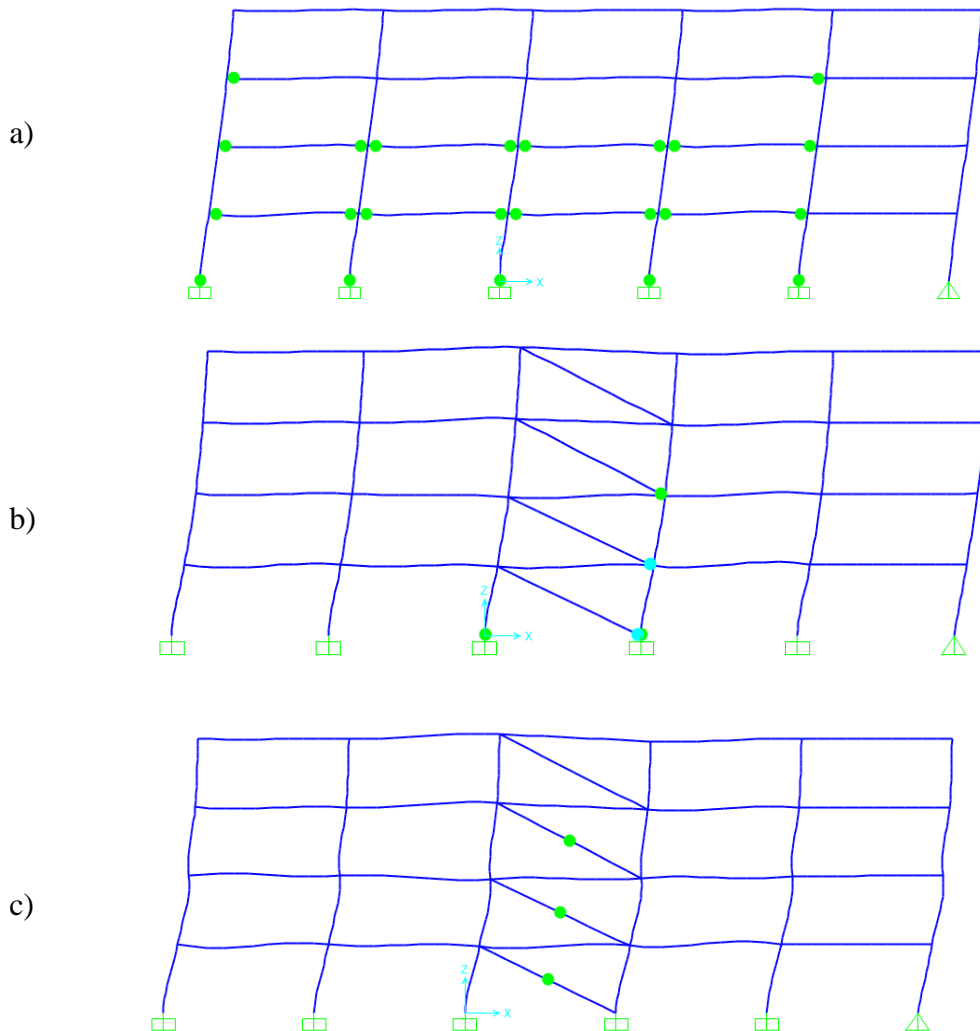


**Figure 4.10.** Last state of Plastic hinges under RSN 983 ground motion for all 4-story frames. **a)** MRF **b)** BF **c)** FDBF



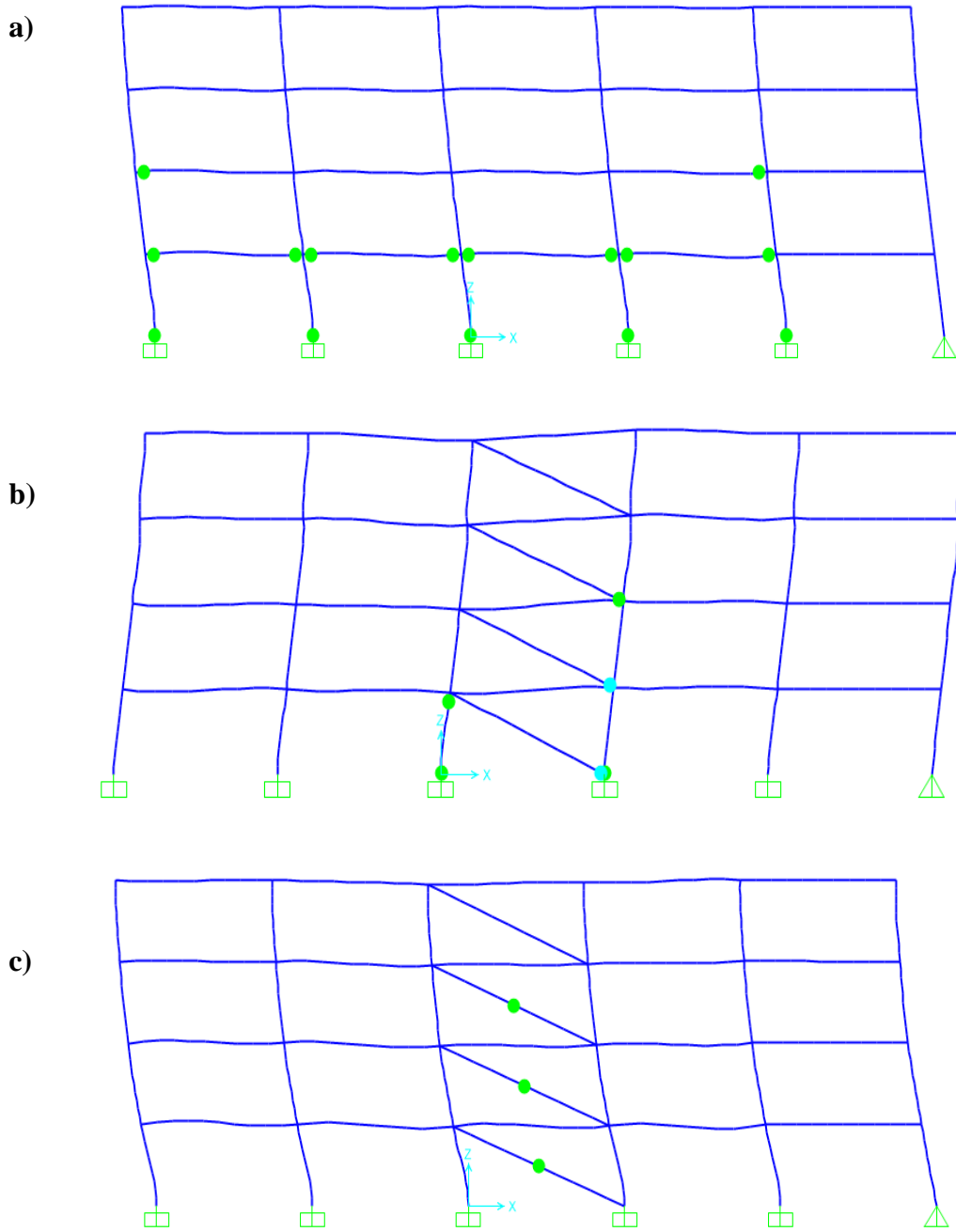


**Figure 4.11.** Last state of plastic hinges under RSN 1013 ground motion for all 4-story frames. **a)** MRFB **b)** BF **c)** FDBF

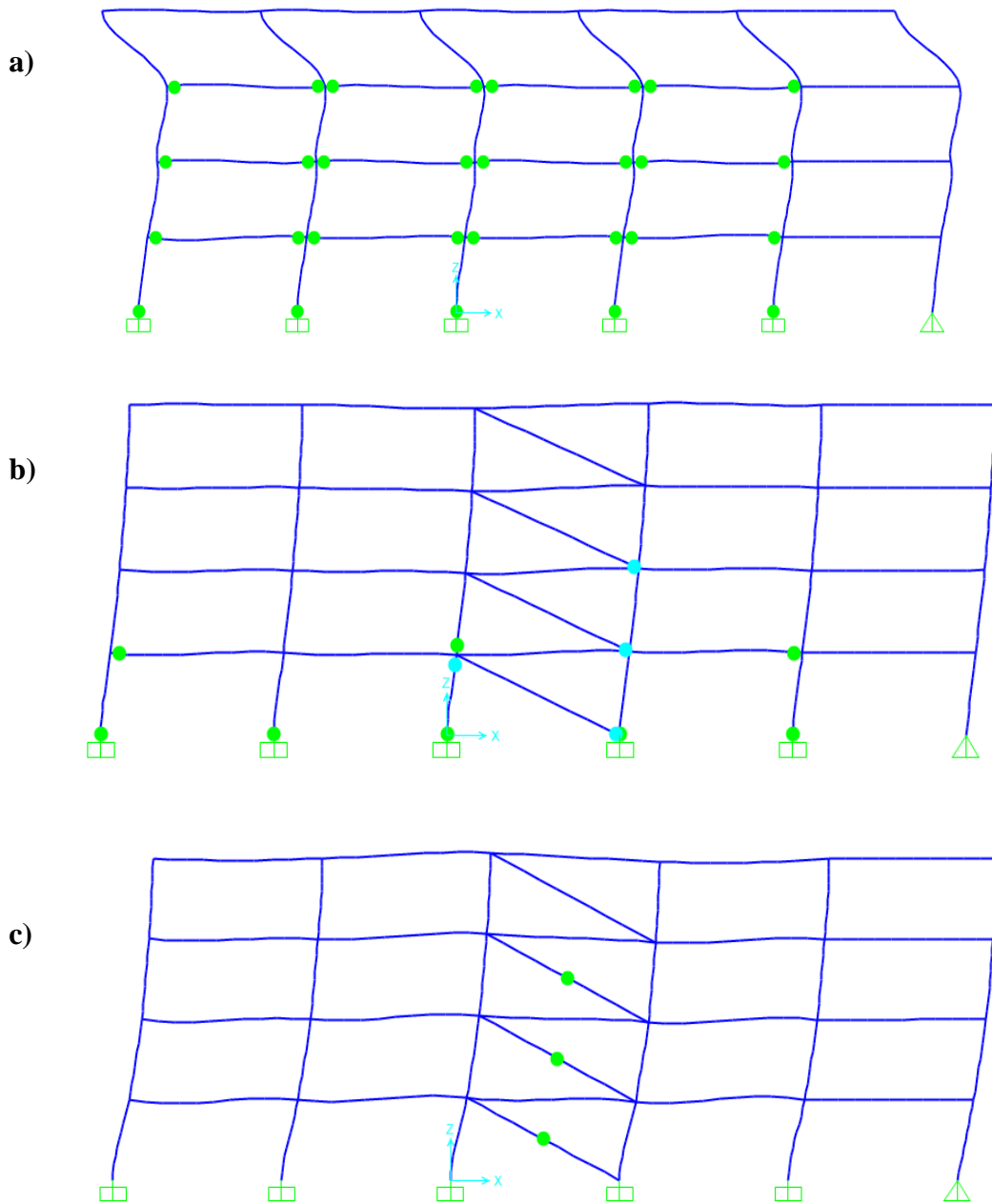


**Figure 4.12.** Last state of plastic hinges under RSN 8164 ground motion for all 4-story frames. **a)** MRF **b)** BF **c)** FDBF

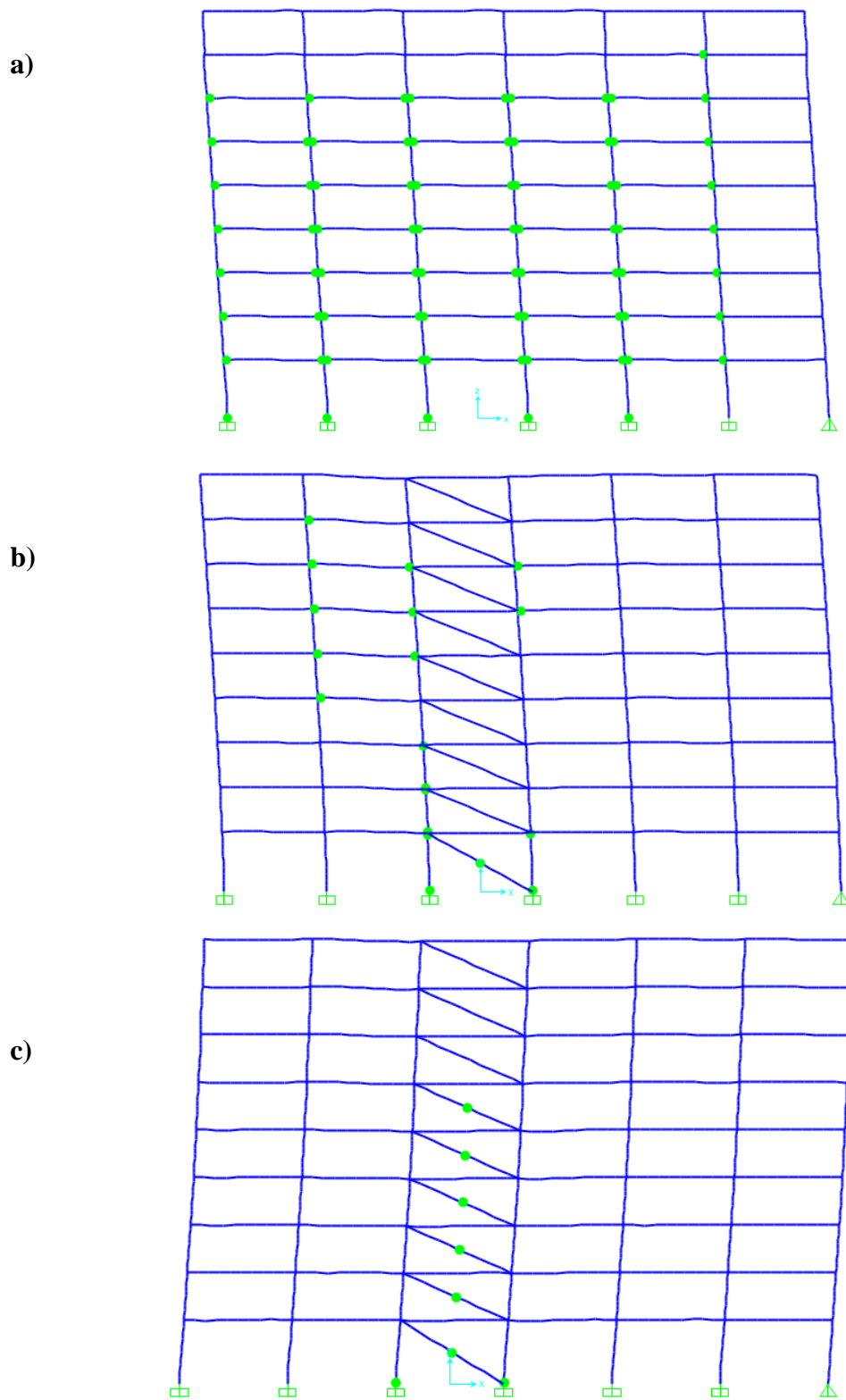


**Figure 4.13.** Last state of plastic hinges under RSN 983 ground motion for all 9-story frames. **a)** MRF **b)** BF **c)** FDBF

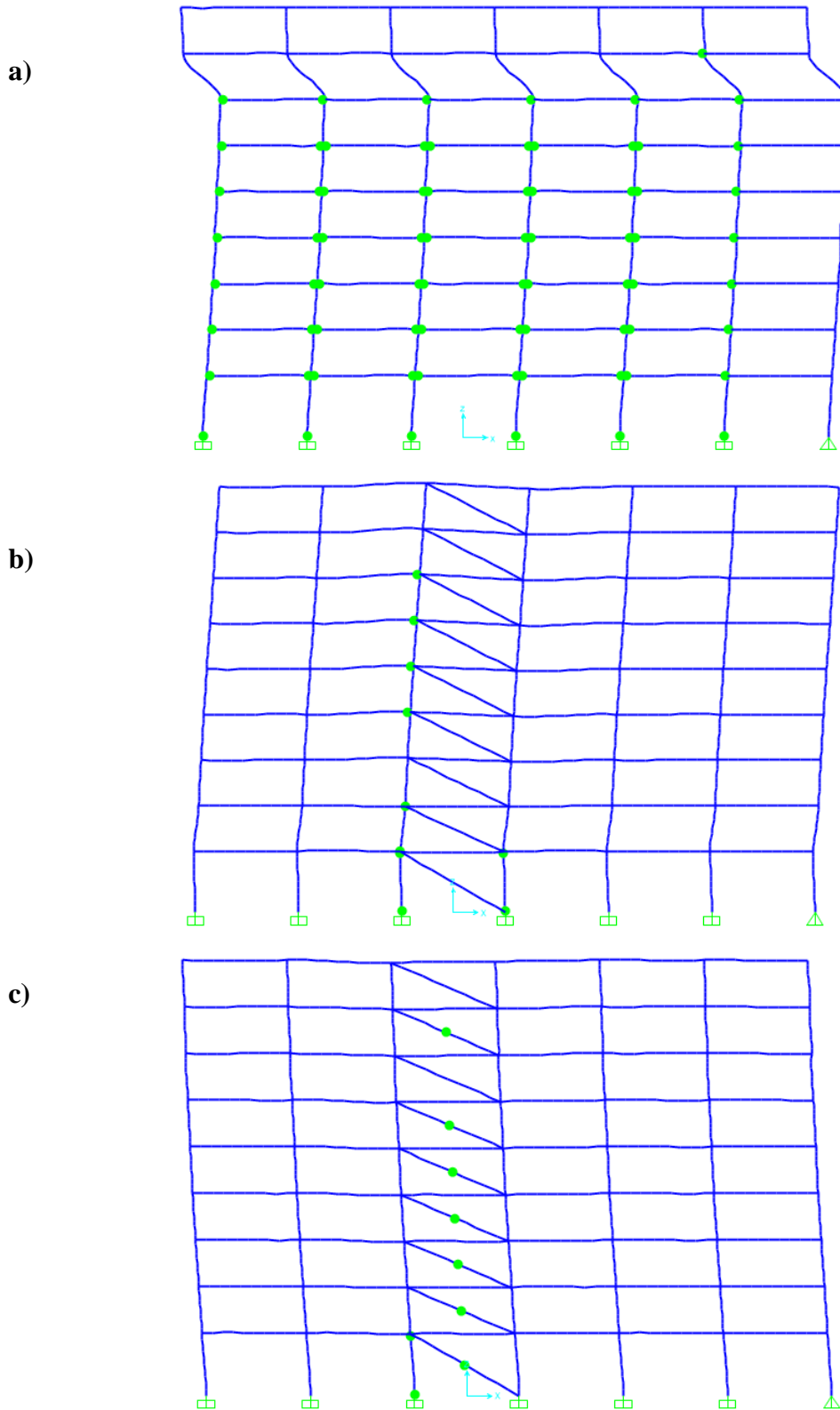


**Figure 4.14.** Last state of Plastic hinges under RSN 1111 ground motion for all 9-story frames. a) MRF b) BF c) FDBF

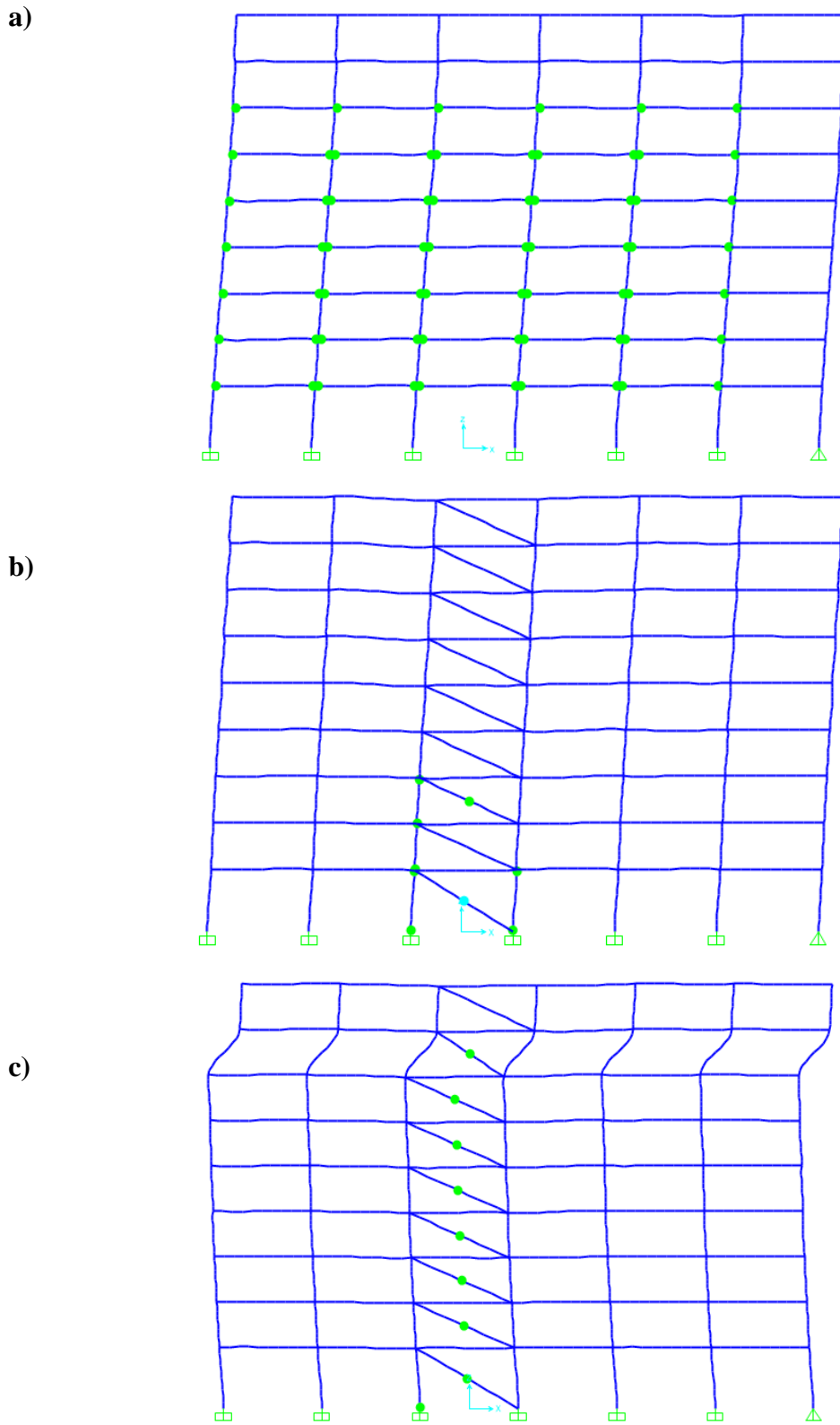


**Figure 4.15.** Last state of Plastic hinges under RSN 4456 ground motion for all 9-story frames. **a)** MRF **b)** BF **c)** FDBF

## 5. CONCLUSION

Focusing on case studies, this investigation was aimed at applying the nonlinear dynamic analysis (time-history analysis) as well as nonlinear static (pushover) analysis for evaluating the performance of moment resisting frame MRF, Braced frame BF, and friction damped braced frame FDBF to check the effectiveness in controlling deformations and improving the seismic performance of the system with the addition of friction damped braces. Two steel structures were chosen for this purpose, consisting of four and nine floors, with four and five bays, respectively and designed according to deformation-based design approach. The results of the study can be summarized as follows.

- The approach proposed by [Baktash 1989] for calculating slip load values for each FDB in the 4 and 9 story systems was followed in this investigation. This approach claims that when the shear resisted by the damped brace  $V_b$  is equivalent to that of the frame without bracing  $V_f$ , the friction damped bracing system dissipates the most energy.
- The study showed the comparison of the period and frequency values for all frames. It was clear that period values of the structure oscillations have been shifted to a lower value due to adding friction dampers to the system. The reduction is equal to 60% in the period for the first mode in 4-story FDBF and about 52% for the first mode in 9-story FDBF which is a result of the increase in frame stiffness.
- By conducting several ground motions on systems in time history analysis, the comparison of top displacement of 4-story system values under RSN 983 ground motion showed a 54% reduction in top displacement of BF compared to the MRF. Additionally, after incorporating FDBs into the MRF system, the displacement further reduced by approximately 77%.
- For the 9-story frames, the roof displacement values under same ground motion resulted in a 52% reduction for the BF system and a reduction of about 58% for the FDBF system compared to the MRF.

- The comparison of story drifts for the 4-story system showed that the FDBF system exhibited a maximum relative story drift value of 0.6%, which was a significant reduction of approximately 60% compared to the results obtained from the MRF analysis. In contrast, the MRF and BF systems had higher maximum relative story drift values of about 1.5% and 0.9% respectively.
- For the story drift values in 9-story frames, the FDBF system showed a maximum relative story drift value of 0.7%, which was again a reduction of about 60% compared to the MRF system. The MRF system recorded a maximum relative story drift value of 1.8%, while the BF system had a value of 1.0%. Notably, the story drift values in the FDBF system were more evenly distributed from the lower story to the upper story.
- The comparison of average values of shear forces under different ground motions for all frames showed that the shear force values of FDBF are approximately in the middle between MRF system and BF due to the addition of friction dampers. It also appears from the graphs that the shear forces decrease more regularly as we go up to higher floors in the FDBF systems.
- The state of plastic hinges showed that by the addition of FDBs to MRF systems, beams and columns are protected from yielding and hinge formation during the seismic events.
- The comparison of pushover curves illustrated that there was a systematic increase in the base shear value as a result of the addition of friction dampers. The increase was about twice the base shear values compared to MRF, while the BF systems showed a greater increase and then a collapse of the structural elements after the significant increase in base shear.

It is clear that the 4-story and 9-story friction damped systems had better seismic performance than the MRF and BF systems, in terms of the roof displacements, story drifts and plastic hinges deformation.

Friction dampers are widely used to control the kinetic energy of moving objects as they are the most effective, reliable, and inexpensive in cost.

## REFERENCES

- Pall, A. S., & Pall, R. (1996, June). Friction-dampers for seismic control of buildings—a Canadian experience. In Eleventh world conference on earthquake engineering, Acapulco, Mexico.
- Filiatrault, A., & Cherry, S. (1987). Performance evaluation of friction damped braced steel frames under simulated earthquake loads. *Earthquake spectra*, 3(1), 57-78
- Fitzgerald, T. F., Anagnos, T., Goodson, M., & Zsutty, T. (1989). Slotted bolted connections in aseismic design for concentrically braced connections. *Earthquake spectra*, 5(2), 383-391.
- Federal Emergency Management Agency (FEMA), 1997. “Prestandard and Commentary for the Seismic Rehabilitation of Buildings”, FEMA-273 Washington, D.C.
- Federal Emergency Management Agency (FEMA), 2000. “Prestandard and Commentary for the Seismic Rehabilitation of Buildings”, FEMA-356, Washington, D.C.
- American Society of Civil Engineers. (2014). Seismic evaluation and retrofit of existing buildings. American Society of Civil Engineers.
- Butterworth, J. W., & Clifton, G. C. (2000, January). Performance of hierarchical friction dissipating joints in moment resisting steel frames. In *Proceedings of 12th World Conference on Earthquake Engineering*.
- Xie, R. (2019). Improved modelling and implementation guidance of energy dissipation devices.
- Arat, M. F. (2020). Performans Tabanlı Plastik Tasarım Yönteminin Şekil Değiştirmeye Göre Tasarım Yöntemiyle Kıyaslanması (Doctoral dissertation, Bursa Uludag University (Turkey)).
- Ramhormozian, S., Clifton, G. C., MacRae, G. A., & Davet, G. P. (2017). Stiffness-based approach for Belleville springs use in friction sliding structural connections. *Journal of Constructional Steel Research*, 138, 340-356.
- Khoo, H. H., Clifton, C., MacRae, G., Zhou, H., & Ramhormozian, S. (2015). Proposed design models for the asymmetric friction connection. *Earthquake Engineering & Structural Dynamics*, 44(8), 1309-1324.
- Yeung, S., Zhou, H., Khoo, H., Clifton, G. C., & MacRae, G. (2013, April). Sliding shear capacities of the asymmetric friction connection. In *New Zealand Society of Earthquake Engineering Conference*. Wellington, New Zealand.
- Atam, E. (2018). Friction damper-based passive vibration control assessment for seismically-excited buildings through comparison with active control: A case study. *IEEE access*, 7, 4664-4675.



Towashiraporn, P., Park, J., Goodno, B. J., & Craig, J. I. (2002). Passive control methods for seismic response modification. *Progress in Structural Engineering and Materials*, 4(1), 74-86.

Gelb Acevedo, M. N. (2014). Influence of the mechanical properties of friction dampers on the seismic response of steel frame structures.

Ahmet Hilmi Deringöl (2013). Effect of friction dampers on seismic performance of buildings

Pasquin, C., Leboeuf, N., Pall, R. T., & Pall, A. (2004, August). Friction dampers for seismic rehabilitation of Eaton's building, Montreal. In 13th world conference on earthquake engineering (pp. 1-2).

Pall, A. (2004, August). Performance-based design using pall friction dampers-an economical design solution. In 13th World Conference on Earthquake Engineering, Vancouver, BC, Canada (Vol. 71).

Cherry, S., & Filiatrault, A. (1993). Seismic response control of buildings using friction dampers. *Earthquake Spectra*, 9(3), 447-466.

Mualla, I. H., & Belev, B. (2002). Performance of steel frames with a new friction damper device under earthquake excitation. *Engineering Structures*, 24(3), 365-371.

Kim, J., Choi, H., & Min, K. W. (2011). Use of rotational friction dampers to enhance seismic and progressive collapse resisting capacity of structures. *The structural design of tall and special buildings*, 20(4), 515-537.

Jarrahi, H., Asadi, A., Khatibinia, M., & Etedali, S. (2020). Optimal design of rotational friction dampers for improving seismic performance of inelastic structures. *Journal of Building Engineering*, 27, 100960.

Pall, A. S., & Marsh, C. (1982). Response of friction damped braced frames. *Journal of the Structural Division*, 108(6), 1313-1323.

Gong, E. M. (2004). Estimating seismic performance of friction damped braced frames by pushover analysis (Doctoral dissertation, Concordia University).

Baktash, P. (1989). Friction damped braced frames (Doctoral dissertation, Concordia University).

Blebo, F. C. (2013). Parametric study of seismic-resistant friction-damped braced frame system (Doctoral dissertation, University of Akron).

Blebo, F. C. (2015). Damage-free seismic-resistant self-centering friction-damped braced frames with buckling-restrained columns. The University of Akron.

Adam, C., & Ziegler, F. (1999, September). Dynamics of friction damped braced frames with secondary structures. In International Design Engineering Technical Conferences and Computers and Information in Engineering Conference (Vol. 80395, pp. 2105-2115). American Society of Mechanical Engineers.

Filiatrault, A. (1988). Seismic design of friction damped braced steel plane frames by energy methods (Doctoral dissertation, University of British Columbia).

Dowdell, D. J. and Cherry, S. (1996), 'On Passive and Semi active Friction Damping for Seismic Response Control of Structures', Proc. 11th World Conference on Earthquake Engineering, Acapulco, Mexico, June 23 - 28, 1996, CD-Rom, Paper 957:8p.

Chopra, A. K., & Goel, R. K. (2001). A modal pushover analysis procedure to estimate seismic demands for buildings: theory and preliminary evaluation. PEER 2001/03.

SAP2000 v23.0.0 2021. Structural Analysis Program, Computers and Structures Inc., California. <https://www.csiamerica.com/products/sap2000> (Date of access: 20.01.2022)

Allahabadi, R. and Powell, G.H. (1988), 'DRAIN-2DX user guide', Report No.UCB/EERC-88/06, Earthquake Engineering Research Center, University of California, Berkeley, Calif.

Chintanapakdee, C., & Chopra, A. K. (2003). Evaluation of modal pushover analysis using generic frames. *Earthquake engineering & structural dynamics*, 32(3), 417-442.

Gong, E. M. (2004). Estimating seismic performance of friction damped braced frames by pushover analysis (Doctoral dissertation, Concordia University).

Fajfar, P. (2018). Analysis in seismic provisions for buildings: past, present and future. In *Recent Advances in Earthquake Engineering in Europe: 16th European Conference on Earthquake Engineering-Thessaloniki 2018* (pp. 1-49). Springer International Publishing.

Kreslin, M., & Fajfar, P. (2012). The extended N2 method considering higher mode effects in both plan and elevation. *Bulletin of Earthquake Engineering*, 10, 695-715.

Rosenblueth, E., & Herrera, I. (1964). On a kind of hysteretic damping. *Journal of the Engineering Mechanics Division*, 90(4), 37-48.

Zorlu, M., Akbaş, B., Shen, J.J., Şeker, O. 2018. Contribution of gravity frames to seismic performance of steel moment resisting frames. *International conference on earthquake engineering and seismology, 2018, Eskişehir*.

TSCB. 2018. Turkish Seismic Code for Buildings. The Disaster and Emergency Management Presidency of Turkey, Ankara.

PEER. 2006. Pacific Earthquake Engineering Research Center, PEER Strong Motion Database. Retrieved from <https://ngawest2.berkeley.edu> (Access Date: 05.04.2020).

## RESUME

Name Surname : Shamsuddin Mahmoud SABOUNI  
Place and Date of Birth :  
Foreign Languages : English & Turkish

Education Status  
High School : Khadem AL-Haramen Secondary School  
Bachelor's : Qassim University / 2013-2018

Work Experience :

Contact (e-mail) :

Publications :